
IMAGE: A MAP OF THE STARS OF THE ORION CONSTELLATION

Print ISSN: 2631-8490 Online ISSN: 2631-8504

# JournalPreview

London Journal of Research in Science: Natural and Formal
Volume 23 | Issue 10 | Compilation 1.0

Great Britain Journals Press

WWW.JOURNALSPRESS.COM

# Journal Content
## In this Issue

Great Britain Journals Press

# Antihyperlipidemic Activity of Rhynchosia Beddomei whole Plant: An in Vitro, in Vivo and in Silico Approach

*N V L Suvarchala Reddy, Ganga Raju M, M, Mamatha, M. Lakshmi Madhuri Shabnam Kumari Thakur, Pavani K & G. Kinnera Ratnasri*

## ABSTRACT

Obesity and hyperlipidemia are two widespread and difficult health issues that affect people all over the world. In these situations, elevated blood lipid levels are risk factors for atherosclerosis, coronary artery disease, and cerebral vascular disease. The goal of the current investigation was to evaluate the phytoconstituents' inhibitory effects on in vitro HMG-CoA reductase, in vivo HFD-induced hyperlipidemia, and dexamethasone-induced hyperlipidemia. High cholesterol diet was prepared by mixing cholesterol 2%, sodium cholate 1% and coconut oil 2%, with powdered chow diet which was prepared as pellets was placed in the cage and administered for 20 days. Dexamethasone, a glucocorticoid excess is known to evoke plasma lipid elevation in the dose of 10 mg/kg/day, s.c. was administered to Wistar rats for 8 days. The in vitro assessment of HMG -CoA reductase activity indicated an IC50 value of 150 and 75 µg/mL by the extract and a standard drug (Pravastatin), respectively. Additionally, an in-silico evaluation was made using appropriate docking software and results also indicated as significant interactions of the identified compounds with the target enzyme.

*Keywords:* NA

*Classification:* UDC Code: 615.322

*Language:* English

Great Britain Journals Press

LJP Copyright ID: 925610
Print ISSN: 2631-8490
Online ISSN: 2631-8504

London Journal of Research in Science: Natural and Formal

Volume 23 | Issue 10 | Compilation 1.0

# Antihyperlipidemic Activity of *Rhynchosia Beddomei* whole Plant: An *in Vitro*, *in Vivo* and *in Silico* Approach

N V L Suvarchala Reddy[α], Ganga Raju M[σ], M, Mamatha[ρ], M. Lakshmi Madhuri [CO]
Shabnam Kumari Thakur[¥], Pavani K[§] & G. Kinnera Ratnasri[χ]

## ABSTRACT

*Obesity and hyperlipidemia are two widespread and difficult health issues that affect people all over the world. In these situations, elevated blood lipid levels are risk factors for atherosclerosis, coronary artery disease, and cerebral vascular disease. The goal of the current investigation was to evaluate the phytoconstituents' inhibitory effects on in vitro HMG-CoA reductase, in vivo HFD-induced hyperlipidemia, and dexamethasone-induced hyperlipidemia. High cholesterol diet was prepared by mixing cholesterol 2%, sodium cholate 1% and coconut oil 2%, with powdered chow diet which was prepared as pellets was placed in the cage and administered for 20 days. Dexamethasone, a glucocorticoid excess is known to evoke plasma lipid elevation in the dose of 10 mg/kg/day, s.c. was administered to Wistar rats for 8 days. The in vitro assessment of HMG -CoA reductase activity indicated an IC50 value of 150 and 75 µg/mL by the extract and a standard drug (Pravastatin), respectively. Additionally, an in-silico evaluation was made using appropriate docking software and results also indicated as significant interactions of the identified compounds with the target enzyme. Treatment of rats with the ethanolic extract of Rhynchosia beddomei whole plant resulted in significant ($p<0.05$) reductions in total cholesterol, LDL cholesterol, VLDL cholesterol, and triglyceride. It can be illustrating that the methanolic extract of Rhynchosia beddomei whole plant contains potent bioactive phytocompounds might be inhibit HMG – CoA reductase and have reduction potential of atherogenic index.*

*Author:* Department of Pharmacology, Gokaraju Rangaraju College of Pharmacy, Nizampet Village, Bachupally, Hyderabad, Telangana State.

London Journal of Research in Science: Natural and Formal

## I. INTRODUCTION

Hyperlipidaemia, commonly known as hypercholesterolemia or hyperlipoproteinemias, is a condition when there are abnormally high levels of fats in the blood. The structure and functionality of blood-circulating cholesterol is complex. According to (Ankur *et al.*, 2012), TGs are quickly recycled, deposited in adipocytes, absorbed from the intestine, or processed in hepatic tissue. When endothelial cells begin to suffer damage from atherosclerotic abrasion, cholesterol crystals are discovered. Increased blood lipids (LDL) have been proven to cause atherosclerosis, while epidemiological data has shown that high HDL levels have a protective effect. The greatest risk factor for artery hardening and narrowing is hyperlipidemia. Additional issues include thrombosis, elevated blood pressure, weight gain, and T2DM (Desu and Saileela, 2013). High fat diet and Dexamethasone are used in induction of hyperlipidaemia and Pravastation, Atorvastatin serves as standard in our present study. The healthcare system is structured in such a way that natural remedies are now widely perceived as inferior or something that people use when they cannot afford modern medicine.

*Rhynchosia beddomei* called as adavi kandi and vendaku, found in dry deciduous forests. It is rampant in South India; originate in AP and Karnataka. The leaves of *Rhynchosia beddomei* have abortifacient, antibacterial, antifungal, antidiabetic hepatoprotective properties and are also used for healing

wounds, cuts, boils and rheumatic pains by adivasi tribes. Root decoction is applied on chronic sores to keep off infection due to airborne diseases. A liniment prepared from the root is applied to reduce the pain near swollen wounds. The crushed stem parts are boiled in the sesame oil and used externally to cure sprains. The leaf paste is used as an antidote to treat insect bites. The aim of our study is to evaluate anti-hyperlipidemic activity of the whole plant extract of *Rhynchosia beddomei* in Wistar Albino rats and to execute *in-silico* analysis.

## II. MATERIALS AND METHODS

All the chemicals used in the present study were procured from Sigma-Aldrich, Loba Chemie, Merck, Sdfine-Chem, Himedia and Spectrochem.

### *2.1 Plant collection & drying*

*Rhynchosia beddomei* whole plant procured, prepared and referred for certification which were verified by Dr. K. Madhava Chetty, botanist, S.V University, Tirupati. Whole plant, cleaned under running water to remove debris and dried in shade. The dried plant material is then made into a coarse powder and was subjected to further steps.

### *2.2 Preparation of Plant Extract*

The powdered plant material was successively extracted in 500 ml of methanol using Soxhlet extraction and plant material was suspended in the round bottomed flask containing extraction solvent. This was then equipped by a condenser and flask was then heated; active constituents of extract get into the fluid. The finale of the extraction process source was filtered. The excess was vaporized and extracts were then kept in desiccators to remove remaining moisture, if extant, and finally stored in air tight ampoules at 4°C until used.

### *2.3 Preliminary phytochemical screening*

Preliminary phytochemical screening of the methanolic whole plant extract of *R. beddomei* (MERB) was qualitatively tested for the presence of phytochemical constituents such as alkaloids, flavonoids, terpenoids, phenols, tannins etc.,

### *2.4 Antihyperlipidemic Activity*

#### *2.4.1 In vitro HMG-CoA reductase activity*

The concentration of the purified human enzyme stock solution was 0.52–0.85 mg protein/mL. Pravastatin was castoff as reference. To characterize HMG-CoA reductase inhibition under defined assay conditions, reactions containing 4 µL of NADPH (to obtain a final concentration of 400 µM) and 12 µL of HMG-CoA substrate (to obtain a final concentration of 400 µM) in a final volume of 0.2 mL of 100 mM potassium phosphate buffer, pH 7.4 (containing 120 mM KCl, 1 mM EDTA, and 5 mM DTT), were initiated (time 0) by the addition of 2 µL of the catalytic domain of human recombinant HMG-CoA reductase and incubated at 37 °C in presence or absence (control) of 1 µL aliquots of drugs dissolved in DMSO. The rates of NADPH consumed were monitored every 20 sec up to 15 min spectrophotometrically. $IC_{50}$ value was calculated and the % inhibitory enzymatic activity was calculated using the formula (Suvarchala *et al.,* 2015).

### 2.5 In vivo Anti-hyperlipidemic Activity

#### 2.5.1 High fat diet induced hyperlipidaemia in rats

High cholesterol diet was prepared by mixing cholesterol 2%, sodium cholate 1% and coconut oil 2%, with powdered standard animal food. The diet which was prepared as pellets was placed in the cage and administered for 20 days. Adult Wistar albino rats were administered with corresponding treatments for one month. They were divided into 5 groups with 6 animals per group. Study design of High fat diet induced hyperlipidaemia method is Group –I serves as Control (Normal saline) were as Group –II received HFD, Group –III received HFD and methanolic extract of *Rhynchosia beddomei* (300mg/kg, *p.o*) and Group – IV received HFD and atorvastatin (10 mg/kg/day *p.o*) (Suvarchala *et al.*, 2015).

#### 2.5.2 Biochemical investigations for body fat

The serum triglycerides and HDL (High Density Lipoproteins) and total cholesterol were measured using span diagnostic kit. TC, TG and High-Density Lipoproteins profiles were estimated using standard monograph.

#### 2.5.3 Measurement of cardiac disorder threat issue

Atherogenic index (AI), which is a measure of the atherogenic potential of an agent, was calculated using the formula and the results were tabulated.

Atherogenic Index (AI) = LDL - cholesterol/HDL – cholesterol

$$\% \text{ Protection} = \frac{\text{AI of control-AI of treated group}}{\text{Atherogenic Index of control}} \times 100$$

#### 2.5.4 Dexamethasone-induced hyperlipidaemia in rats

To induce hyperlipidaemia, dexamethasone, (a glucocorticoid excess is known to evoke plasma lipid elevation) in the dose of 10 mg/kg/day, *s.c.* was administered to Wistar rats for 8 days and animals were divided into five groups each group containing six rats. After the induction of hyperlipidaemia, MERB were given to the rats for 8 days at a dose of 300 mg/kg and on 9$^{th}$ day, after overnight fasting blood was collected from retro-orbital plexus for the study of biochemical parameters. Study design of High fat diet induced hyperlipidaemia method is Group–I serves as Control (Normal saline) were as Group –II received dexamethasone 10 mg/kg, b.w., s.c., Group –III received dexamethasone 10 mg/kg, b.w., *s.c.* and methanolic extract of *Rhynchosia beddomei* (300 mg/kg, *p.o*) and Group – IV received HFD and atorvastatin (10 mg/kg/day *p. o*) (Suvarchala *et al.*, 2015).

### 2.6 In silico analysis

#### 2.6.1 Molecular Docking Studies

Molecular docking is an attractive scaffold to understand drug bimolecular interactions for rational drug design and discovery. Molecular docking generates different possible adduct structures that are ranked and grouped together using a scoring function in the software. The main objective of molecular docking is to attain ligand-receptor complex with optimized conformation and with the intention of possessing less binding free energy (Suvarchala *et al.,* 2021). Molecular docking performed with mCule online tool.

#### 2.6.1.1 Structure based drug design

Initially the protein downloaded in PDB format was prepared in discovery studio by generating attributes of sphere. Water molecules present in both the chains are removed. Later molecules are drawn using chemdraw/Chemsketch in mol format. Protein and ligand were docked against proteins like 3ASX, 6Q2T and 7S5G. Docking indicates that some of our compounds, docked with protein of Squalene synthase Inhibitor (PDB ID: 3ASX), Lanosterol 14 alpha demethylase Inhibitor (PDB ID: 6Q2T) and PCSK9 Inhibitor (PDB ID: 7S5G)

#### 2.6.1.2 Docking results visualization

The resulting docking poses were visualized through discovery studio. The best docked structures were chosen using glide score function. The more negative the glide score the more favourable the binding. Additionally, the docked ligand poses were visualized and the different ligand receptor interactions were studied (Ganga raju *et al.,* 2021).

### 2.6.2 Ramachandran plot

The docked proteins of Squalene synthase Inhibitor (PDB ID: 3ASX), Lanosterol 14 alpha demethylase Inhibitor (PDB ID: 6Q2T) and PCSK9 Inhibitor (PDB ID: 7S5G) protein were validated and evaluated by using procheck by calculating the Ramachandran plot to access the quality of the model by looking into the allowed and disallowed regions of the plot (Ganga raju *et al.,* 2022). The Ramachandran plot shows the phi-psi torsion angles for all residues in the ensemble (except those at the chain termini). The colouring/shading on the plot represents the different regions described by Morris. the darkest areas (here shown in *red*) correspond to the "core" regions representing the most favourable combinations of phi-psi values.

### 2.7 Statistical analyses

The Results were expressed as the AM ± S.E.M. The significance of the results was calculated using ANOVA and Dunnett's t-test and results were deliberated statistically noteworthy when significant $p<0.01$, $p<0.05$ ns- non significant.

## III. RESULTS AND DISCUSSION

### 3.1 Preparation of Rhychosia beddomei methanolic extract

The methanolic extract of *Rhychosia beddomei* was prepared by soxhlation technique. The percentage yield of the extract was calculated by using the following formula.

$$\% \text{ yield of extract} = \frac{\text{Amount of extract obtained (grams)}}{\text{Amount of the powder used (grams)}} \times 100$$

$$= 35.43\%. \quad w/w.$$

### 3.2 Preliminary phytochemical screening

Crude extract was then subjected to preliminary phytochemical screening of *Rhynchosia beddomei* showed the presence of alkaloids, glycosides, steroids, flavonoids, carbohydrates, proteins and tannins.

### 3.3 Invitro antihyperlipidemic Activity

#### 3.3.1 In vitro HMG CoA Reductase Inhibitor Activity

The data of percent inhibition and $IC_{50}$ at two dose levels of methanolic extracts of two plants are presented in Table 1 indicated that the % inhibition is increased with increase in dose of plant extract, though proportionate increase was not obtained. Additionally, inhibition data were processed for relative inhibition compared to standard and reported. The processing is done on the lines of expressions of relative bioavailability (%). Higher the relative inhibition, the greater is the inhibition of HMG CoA reduction. In this study, standard is pravastatin. As expected, pravastatin produced inhibition at lower dose (100 µg/mL). Plant extracts also showed appreciable inhibition at greater doses (500 µg/mL). The methanolic extracts of both plants showed same extent of % inhibition of the HMG CoA reduction.

The $IC_{50}$ values of standard and test extracts are compared and the ratio was found to be less by 55% respectively, for MERB.

*Table 1:* In vitro HMG-COA reductase inhibitory activity of MERB

| Test extract/standard | Dose (µg/mL) | Percentage inhibition AM±SEM (n=3) | % Relative inhibition | $IC_{50}$ (µg/mL) |
|---|---|---|---|---|
| Methanolic extract of *Rhynchosia beddomei* | 100 | 43.33 ±0.76 | 33.34 | 150 |
| | 500 | 85 ±0.012 | 73.9 | |
| Pravastatin (Standard) | 100 | 66.86 ± 0.0788 | 100 | 75 |
| | 500 | 100±0.012 | 100 | |

### 3.4 In vivo Antihyperlipidemic Activity

Hyperlipidaemia was induced by giving high cholesterol diet and dexamethasone (10 mg/kg, b.w., *s. c*) and parameters measured were TC, triglyceride, low density lipoproteins, VLDL, high density lipoprotein levels. Atherogenic index and % protection were also measured.

#### 3.4.1 High fat diet (HFD) induced hyperlipidaemia

Rats fed on HFD is a means for the induction of metabolic syndrome features including distinctive visceral adiposity, dyslipidaemia which are typically associated with human obesity. The rat model of diet-induced obesity is often used to investigate the effects of metabolic syndrome ameliorating agents. The data of cholesterol, triglycerides, LDL, VLDL and HDL levels upon the treatment of *Rhynchosia beddomei* methanolic extract at one dose level (300 mg/kg, b.w.) are presented in Table2. When HFD is provided to rats, cholesterol, triglycerides, LDL, VLDL levels increased and HDL level decreased from 80 to 100% within 20 days. MERB were administered and levels decreased within 30 days compared to Disease control group. The standard in the present study is atorvastatin (10 mg/kg, b.w.). As expected, standard produced lower levels of cholesterol, triglycerides, LDL, VLDL and increased HDL levels at 10 mg/kg. The MERB 300 also showed appreciable decrease of cholesterol levels and nearer to the standard value. In the present work, *Rhynchosia beddomei* was reported to contain β-sitosterol and stigmasterol. These might be responsible to lower cholesterol in animals fed with HFD.

*Table 2:* Effect of MERB on cholesterol, triglycerides, LDL, VLDL and HDL in high fat diet induced model

| Groups | Treatment/Standard Dose mg/kg, b.w. | Lipid Profile (mg/dL) AM±SEM | | | | |
|---|---|---|---|---|---|---|
| | | Cholesterol | Triglycerides | LDL | VLDL | HDL |
| I | Control | 104.2±0.47 | 79.83±1.68 | 42.93±0.30 | 15.8±0.33 | 46.83±0.15 |
| II | Cholesterol control | 219.66±0.1$^{a,A}$ | 185.5±1.94 $^{b,A}$ | 162.96 ±0.05 $^{b,A}$ | 34.3±0.16$^{b,A}$ | 31.33±0.6 $^{a,A}$ |
| III | MERB 300 | 112.6±1.7 $^{b,B}$ | 109±1.54 $^{a,B}$ | 48.7±0.6 $^{a,B}$ | 18.1±0.2 $^{b,A}$ | 45.8±0.9 $^{b,A}$ |
| IV | Atorvastatin 10 | 110.3±0.4 | 104.1±1.3 | 46.5±0.02 | 17.83±0.07 | 46.5±0.17 |

In view of reducing cholesterol by plant extracts and other related parameters, TG, LDL, VLDL was further evaluated. When HFD is provided to rats, triglyceride levels were increased by 80 to 100% within 20 days and LDL levels were amplified by 300% within 20 days, VLDL levels were doubled by within 20 days, HDL levels were decreased by 20% within 20 days in disease group. The plant extract was administered, the triglyceride levels, LDL, VLDL levels decreased compared to control, the test samples of significant in $p<0.05$ , compared to standard, the samples have significantly different ($p<0.01$) and HDL increased within 30 days compared to control ($p<0.05$), when compared to standard the samples are significantly different ($p<0.05$).

*Measurement of Cardiac Disorder Threat Issue*

### *3.4.1.1 Atherogenic Index*

The atherogenic index is obtained based on the knowledge of cholesterol, LDL and HDL values. Thus the index was calculated. The data of atherogenic index upon the treatment of plant extracts at one dose level (300 mg/kg, b.w.) shown in figure, indicated that the atherogenic index remained same for the control up to 30 days. When high fat diet is provided to rats, the atherogenic index was increased by 3 times (300%) within 20 days. The differences between control and cholesterol control are significant ($p<0.05$). The plant extracts were administered, the atherogenic index reached the value of control within 30 days, the test samples are significant ($p<0.05$), when compared to standard, the samples are significantly same ($p<0.01$). The lower the atherogenic index, the higher is the hypolipidemic activity (of the test extracts). The standard in the present study is atorvastatin (10 mg/kg, b.w.). As expected, atorvastatin produced lower levels of atherogenic index (1) at a dose level of 10 mg/kg. The plant extract also showed appreciable decrease of atherogenic index and nearer to the standard value ($p<0.05$).

### *3. 4.1.2 Effect on % protection*

The percent protection of heart is considered based on the levels are different parameters evaluated so far. In the calculation of atherogenic index, control and cholesterol control values are not included. But in the calculation of percent protection, control values are also included. % Protection was calculated for the groups treated with MERB 300 mg/kg, b.w. explained in table 3. As observed in the values of atherogenic index, the percent protection is 30 times lower than the standard, when dose-normalized.

*Table 3:* Effect of MERB on % protection in high fat diet induced model

| Groups | Treatment/Standard Dose mg/kg, b.w. | % Protection, AM±SEM, (n=6) |
|---|---|---|
| I | Control | - |
| II | Cholesterol control | - |
| III | MERB 300 | 72.04±0.43 $^{b,A}$ |
| IV | Atorvastatin 10 | 72.6±0.56 $^{b}$ |

*Test groups were compared with control group and standard group. By using Dunnett's t-test significant values are expressed as control group (a=p<0.01, b=p<0.05) and standard (A = p < 0.01, B = p < 0.05), ns- non significant.*

### *3.4.2 Dexamethasone induced hyperlipidaemia*

Dexamethasone, triggering a disproportion in lipid metabolism leading to hyperlipidaemia (Wiesenberg *et al.,* 1998). Hyperlipidaemia was produced by administering dexamethasone (10 mg/kg, b.w., *s. c*). The parameters measured were total cholesterol; triglyceride, LDL, VLDL, HDL levels, atherogenic index and percent protection were also measured. The antihyperlipidemic activity was evaluated for MERB.

The cholesterol, triglycerides, LDL, VLDL and HDL levels upon the treatment MERB at one dose level (300 mg/kg, b.w.) are presented in Table 4 indicated that all levels remained same for the control upto 11 days. When dexamethasone is injected to rats, the cholesterol, TGL, VLDL levels were almost doubled, the LDL levels increased nearly 3½ times and HDL levels were decreased by 5 to 6% within 11 days. The Methanolic extract of *Rhynchosia beddomei* extract were administered, the cholesterol, triglycerides, LDL, VLDL levels decreased and HDL levels increased when compared to control, the results of test samples are significant ($p<0.05$) that indicates the higher is the hypolipidemic activity of the test extract may be due to the presence of phytosterol (Bopanna *et al* 1997). Any lipid reduction (1% cholesterol) produces a 2-3% reduction in CHD risk (Xu *et al* 2005). The standard, atorvastatin (10 mg/kg, b.w.) produced lower levels of cholesterol. In the present work, *Rhynchosia beddomei* was reported to contain β-sitosterol and stigmasterol. These might be responsible for lowering the Lipid levels, though the animals were injected with dexamethasone.

*Table 4:* Effect of MERB on cholesterol, triglycerides, LDL, VLDL and HDL in dexamethasone induced model

| Group | Treatment/Standard Dose mg/kg, b.w. | Lipid Profile (mg/dL) AM±SEM, (n=6) | | | | |
|---|---|---|---|---|---|---|
| | | Cholesterol | Triglycerides | LDL | VLDL | HDL |
| I | Control | 104±0.09 | 79±0.28 | 44±0.09 | 16±0.22 | 47±0.15 |
| II | Cholesterol control | 233±0.93 $^{a,B}$ | 157±0.23 $^{b,A}$ | 176±0.7 $^{b,B}$ | 51±0.7 $^{b,A}$ | 26±0.86 $^{b,B}$ |
| III | MERB 300 | 108±0.92 $^{a,B}$ | 99±0.02 $^{a,A}$ | 57±0.64 $^{a,A}$ | 20±0.21 $^{b,B}$ | 40±0.44 $^{a,A}$ |
| IV | Atorvastatin 10 | 105±0.69 $^{b}$ | 92±0.46 $^{b,B}$ | 53±0.46 $^{b,A}$ | 18±0.5 $^{a,A}$ | 43±0.08 $^{b,A}$ |

Test groups were compared with control group, cholesterol control group and standard group. By using Dunnett's t-test significant values are expressed as control group (a=p<0.01, b=p<0.05), cholesterol control (**= p<0.01, *= p<0.05) and standard (A = p < 0.01, B = p < 0.05), ns- non significant.

*Measurement of cardiac disorder threat issue*

### 3.4.2.1 Effect on atherogenic index (AI)

When dexamethasone is provided to rats, the atherogenic index was increased by 3 times within 10 days. The data of atherogenic index upon the treatment of MERB at one dose level (300 mg/kg, b.w.) are presented in Table 5. Atherogenic index remained the same for the control upto 11 days. When the MERB was administered, the atherogenic index decreased within 11 days, compared to control and values are nearer to the standard value standard,

*Table 5:* Effect of MERB on atherogenic index in dexamethasone induced model

| Group | Treatment/ Standard Dose mg/kg, b.w. | Atherogenic Index AM±SEM, (n=6) |
|---|---|---|
| I | Control | 0.93±0.28 |
| II | Cholesterol control | 5±0.27 [b,A] |
| III | MERB 300 | 1.23±0.11 [a,A] |
| IV | Atorvastatin 10 | 1.09±0.04 [a] |

Test groups were compared with control group, cholesterol control group and standard group. By using Dunnett's t-test significant values are expressed as control group (a=p<0.01, b=p<0.05), cholesterol control (**= p<0.01, *= p<0.05) and standard (A = p < 0.01, B = p < 0.05), ns- non significant.

### 3.4.2.2 Effect on % protection

Percent protection was calculated for the groups treated with MERB 300 mg/kg, b.w. As observed in the values of atherogenic index, the percent protection is 30 times lower than the standard, when dose-normalized.

*Table 6:* Effect of MERB on % protection in dexamethasone induced model

| Groups | Treatment/Standard dose, mg/kg, b.w. | % Protection AM±SEM (n=6) |
|---|---|---|
| I | Control | - |
| II | Cholesterol control | - |
| III | MERB 300 | 81.2±0.41 [a,A] |
| IV | Atorvastatin 10 | 81±0.74 [a] |

*Test groups were compared with control group, cholesterol control group and standard group. By using Dunnett's t-test significant values are expressed as control group (a=p<0.01, b=p<0.05), cholesterol control (**= p<0.01, *= p<0.05) and standard (A = p < 0.01, B = p < 0.05), ns- non significant.*

Dexamethasone induced hyperlipidaemia, the animal model effectively used for evaluating the antihyperlipidemic activity of natural products (Kumar *et al.*, 2007). In the present study, treatment with MERB (300 mg/kg) has reduced the serum cholesterol, triglycerides levels and atherogenic index, in dexamethasone treated animals. The extracts inverted the hyperlipidaemia produced by administration of dexamethasone. The low lipoprotein lipase activity in the liver may be responsible for low degradation of lipoprotein, triglycerides and cholesterol. Hence the hyperlipidemic effect of dexamethasone was found to be reversed by MERB, further this was also found to be comparable with that of atorvastatin. In this work, friedelin is proposed to decrease the TC, TG, and LDL-C and increase the HDL-C levels significantly. The methanolic extract of *Rhynchosia beddomei* contains

phytosterol and flavonoids. The high amount of flavonoids complemented the phytosterols which might be accountable for the hypolipidemic effect. It also improves HDL- cholesterol levels and lower atherogenic index. More specifically the presence of friedelin has the added benefit of stimulating the synergistic effect for eliciting the antihyperlipidemic activities.

### *3.5 In silico analysis*

#### *3.5.1 Molecular docking studies*

*Table 7:* Docking score of chemical constituents and atorvastatin with protein 3ASX, 6Q2T and 7S5G

| Compounds | 3ASX | 6Q2T | 7S5G |
|---|---|---|---|
| Quercitin-7-O-methyl ether | -8.4 | -6.2 | -5.8 |
| Isovitexin | -8.5 | -6.3 | -6.2 |
| 5,7,3',4'-tetrahydroxy 6-c- β -D-glucopyrynosyl flavone | -7.5 | -5.6 | -5.9 |
| Apigenin | -8.2 | -7.0 | -6.0 |
| Vitexin | -8.3 | -6.2 | -5.9 |
| Vicenin | -8.3 | -5.9 | -6.3 |
| Orientin | -8.1 | -5.8 | -5.7 |
| Isoorientin | -7.9 | -6.3 | -6.5 |
| Lucenin | -8.5 | -5.4 | -6.1 |
| Rutin | -8.8 | -5.6 | -5.9 |
| Rhynchosin | -7.9 | -6.9 | -6.0 |
| Biochanin | -7.7 | -7.3 | -6.2 |
| D-Pinitol | -4.8 | -3.5 | -3.9 |
| D-Inositol | -4.6 | -3.5 | -4.0 |
| Atorvastatin | -7.9 | -8.7 | -5.4 |

*G score = glide score, Higher the negativity, the more favourable the binding.*

Hydrophobic bond interactions of ligands with 3ASX, 6Q2T and 7S5G PDB ID: 3ASX

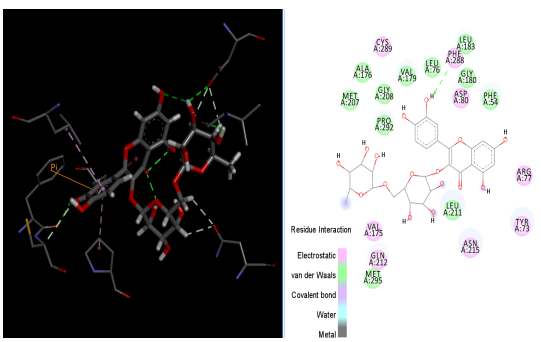


a) Rutin -8.8

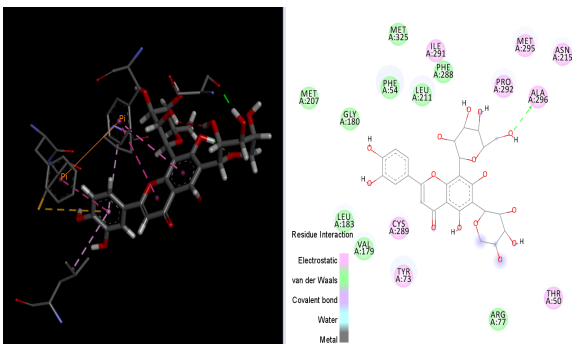


b) Lucenin -8.5

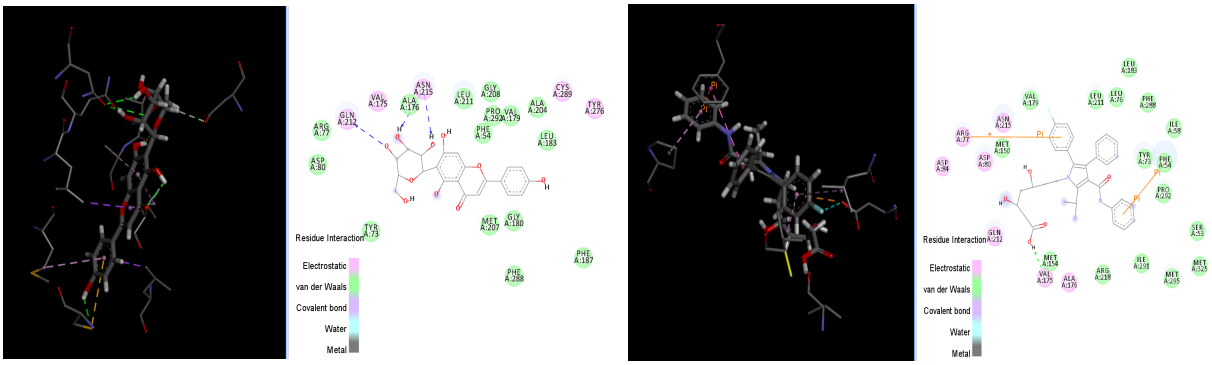


c) Isovitexin -8.5 d) Atorvastatin -7.9

*Figure 3:* 3D & 2D structures of 3ASX protein with Glide scores with interactions PDB ID: 6Q2T

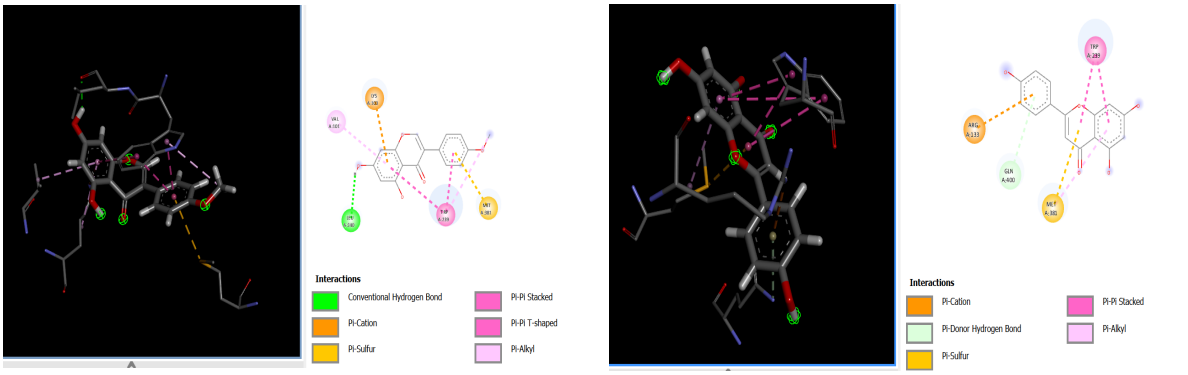


a) Biochanin -7.3 b) Apigenin -7.0

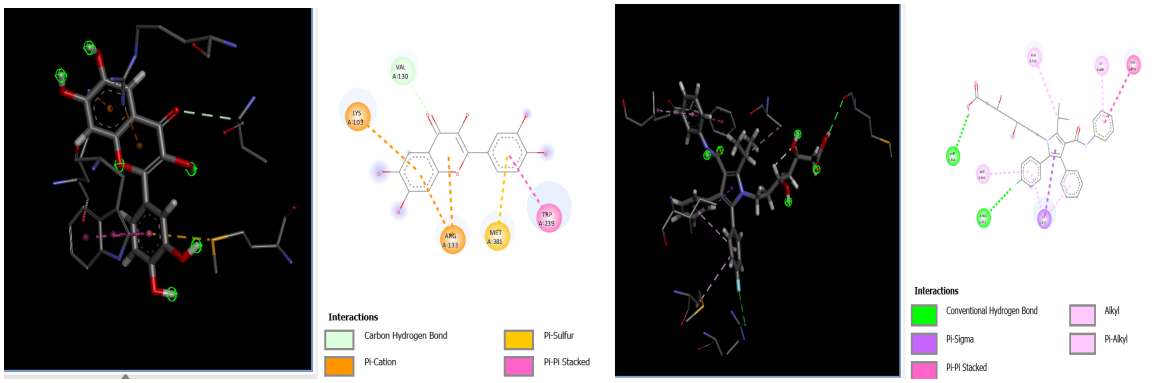


c) Rhynchosin -6.9 d)Atorvastatin -8.7

*Figure 4:* 3D & 2D structures of 6Q2T protein with Glide scores with interactions PDB ID: 7S5G

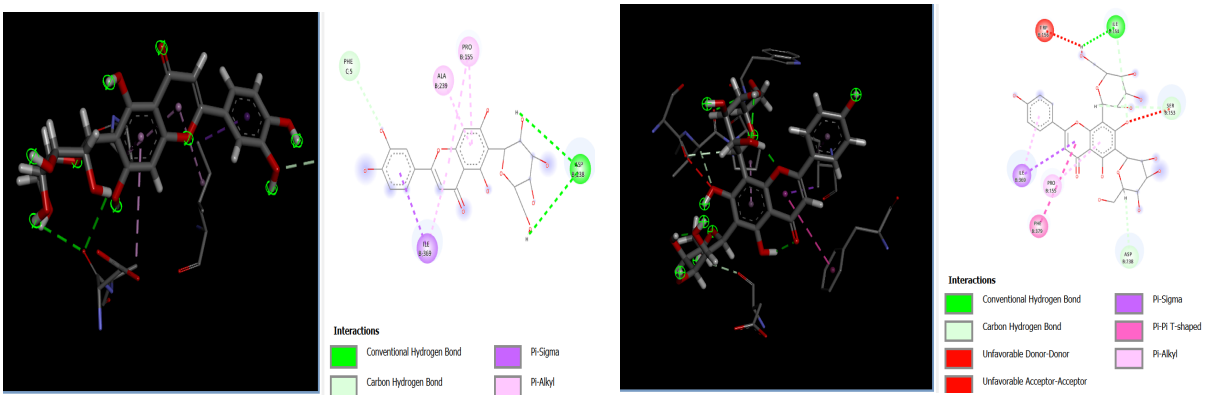


a) Iso orientin -6.5 b) Vicenin -6.3

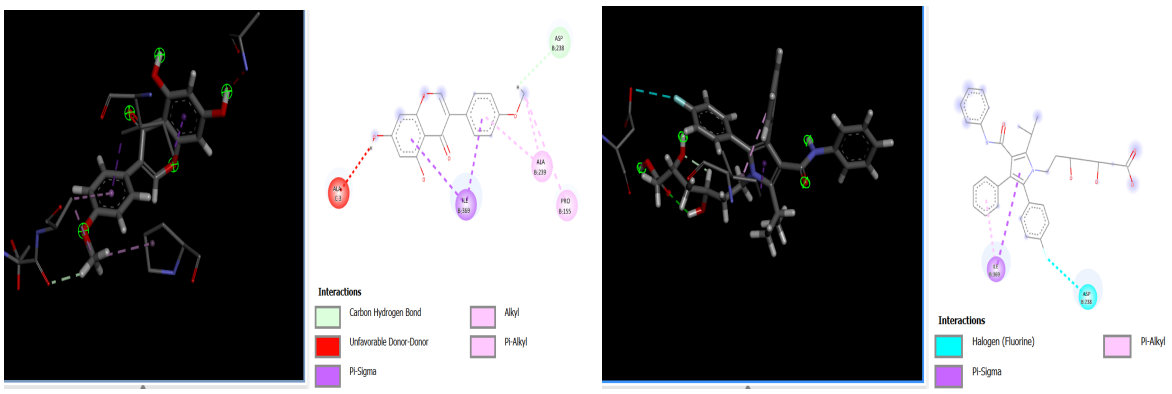


c) Biochanin -6.2 d)Atorvastatin -5.4

*Figure 5:* 3D & 2D structures of 7S5G protein with Glide scores with interactions

The compounds present in MERB, are docked with protein Squalene synthase Inhibitor (PDB ID: 3ASX), Lanosterol 14 alpha demethylase Inhibitor (PDB ID: 6Q2T) and PCSK9 Inhibitor (PDB ID: 7S5G) and Ramachandran plot is analysed. Rutin, Lucenin, Iso vitexin showed good score for protein 3ASX; Biochanin, Apigenin, Rhynchosin for protein 6Q2T, Isoorientin, Vicenin and Biochanin for protein 7S5G shown good docking score when compared to other compounds. Squalene synthase (SQS), a key downstream enzyme involved in the cholesterol biosynthetic pathway, plays an important role in treating hyperlipidemia. Compared to statins, SQS inhibitors have shown a very significant lipid-lowering effect and do not cause myotoxicity (Kourounakis *et al.*, 2020) Lanosterol 14α-demethylase (CYP51A1) is the animal version of a cytochrome P450 enzyme that is involved in the conversion of lanosterol to 4,4-dimethyl cholesta-8 (9),14,24-trien-3β-ol, demethylation of lanosterol has been implicated as a rate-limiting step in the post-squalene portion of cholesterol synthesis, suggesting the reaction as a potential focal point in sterol regulation (DeBose-Boyd, 2008). Proprotein convertase subtilisin kexin type 9 (PCSK9) inhibitors are novel agents indicated for the treatment of hyperlipidemia. Inhibition of PCSK9 produces an increase in surface low-density lipoprotein (LDL) receptors and increases removal of LDL from the circulation (Sible, 2016).

*Ramachandran plot Analysis*

Protein 3ASX, 6Q2T and 7S5G were analysed for Ramachandran plot to know amino acid presence in different regions of respective protein tabulated in table 8 and pictorial representation by figure 6.

*Table 8:* Ramachandran plot status with protein 3ASX, 6Q2T and 7S5G

| Residues | 3ASX | 6Q2T | 7S5G |
|---|---|---|---|
| Most favourable region (%) | 94.8 | 90.9 | 88.4 |
| Additional allowed regions (%) | 5.2 | 8.9 | 11.2 |
| Generously allowed regions (%) | 0.0 | 0.00 | 0.0 |
| Disallowed regions (%) | 0.0 | 0.3 | 0.3 |

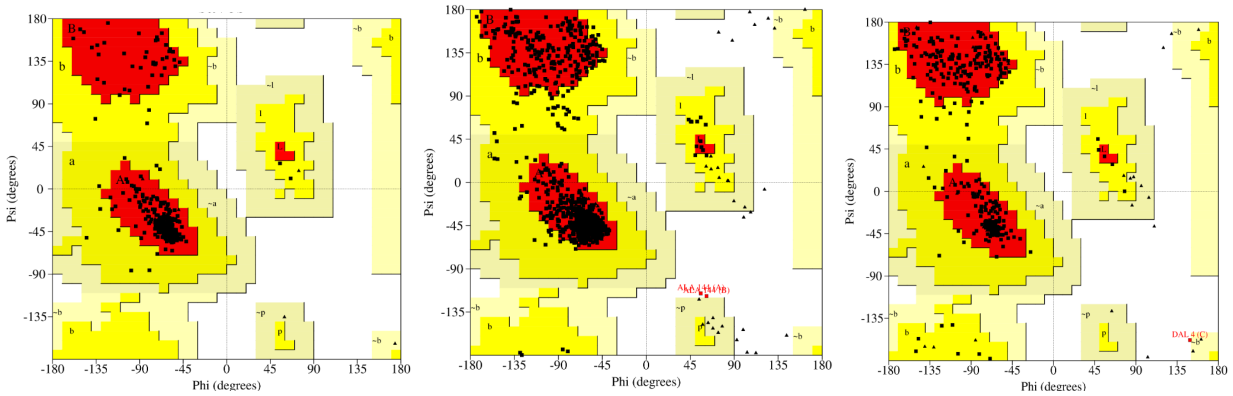


a) 3ASX b) 6Q2T c) 7S5G

## IV. CONCLUSION

Preliminary phytochemical tests of MERB in the present work showed the presence of constituents such as flavonoids, glycosides, sterols, alkaloids and tannins. The whole plant extract of *Rhynchosia beddomei* inhibited HMG-CoA reductase by 43.33% at 100 µg/mL and 85% inhibition at 500 µg/mL. The standard pravastatin was found to possess 65.0% inhibition at 100 µg/mL. Graded response is an encouraging observation. The extract lowered the TC, TG, LDL and VLDL, results were consistently observed in two models, also showed appreciable decrease of atherogenic index and nearer to the standard value. Therefore, more research into the use of a methanolic extract of *Rhynchosia beddomei* whole plant as an alternative therapeutic agent to statins and other medications, but one that has no unwanted side effects, is necessary for the treatment of cardiovascular disorders.

## REFERENCES


1. Ankur R, Nidhi D, Seema R, Amarjeet D and Ashok K. Hyperlipidemia- a deadly pathological condition. *Int J Curr Pharm Res*. 2012; 4(2): pp 15-18.
2. Bopanna KN, Kannan J, Gadgil S, Balaraman R and Rathod SP. Antidiabetic and antihyperlipidemic effects of neem seed kernal powder on alloxan diabetic rabbits. *Ind J Pharmacol*. 1997; 29: pp 162-167.
3. DeBose-Boyd, R. Feedback regulation of cholesterol synthesis: sterol-accelerated ubiquitination and degradation of HMG CoA reductase. *Cell Res* 18, 609–621 (2008). https://doi.org/10.1038/cr.2008.61
4. Desu BSR and Saileela CH. Anti-hyperlipidemic activity of methanolic extract of *Rhinacanthus nasutus*. *Int J Res Pharm Chem*. 2013; 3 (3): pp 708-711.
5. Ganga Raju M, Sony Priyanka G and Suvarchala Reddy NVL. Novel *In Silico* and *In Vivo* Insights of Flavonoids as Anti-Diabetic and Anti-Oxidant in Rodent Models. Indian J Pharm Sci 2022;84 (4):1041-1050
6. Ganga Raju M, Veena Yadav, N V L Suvarchala Reddy V. Natural Compounds as D2 receptor agonist, M4 receptor antagonist and ACHE modulator: Mechanistic and *in silico* modeling studies. Journal of research in medical and dental science. 2021;9(6): 26-35.
7. Kourounakis AP, Bavavea E. New applications of squalene synthase inhibitors: Membrane cholesterol as a therapeutic target. Arch Pharm (Weinheim). 2020 Sep;353(9):e2000085. doi: 10.1002/ardp.202000085. Epub 2020 Jun 18. PMID: 32557793.
8. Kumar BRP, Praveen TK, Nanjan MJ, Karvekar MD and Suresh B. Serum glucose and triglyceride lowering activity of some novel glitazones against dexamethasone-induced hyperlipidaemia and insulin resistance. *Ind J Pharmacol*. 2007; 39: pp 299-302.

9. Sible AM, Nawarskas JJ, Anderson JR. PCSK9 Inhibitors: An Innovative Approach to Treating Hyperlipidemia. Cardiol Rev. 2016 May-Jun;24(3):141-52. doi: 10.1097/CRD.0000000000000102. PMID: 26886466.
10. Suvarchala Reddy NVL, M. Ganga Raju, M. Mamatha, N Nandini. GC-MS analysis, In silico docking studies and diuretic activity of methanolic extract of Citrus medica l. Leaf in Wistar albino rat model. Bull. Env.Pharmacol. Life Sci., Vol 2021;10(3): 42- 50.
11. Suvarchala Reddy NVL, Pooja Raj GB, Ganga Raju M, Sneha J Anarthe. Antihyperlipidemic activity of *Cassia fistula* bark using high fat diet induced hyperlipidemia. International Journal of Pharmacy and Pharmaceutical Sciences. 2015; 7(10): 61-64.
12. Suvarchala Reddy NVL, Swetha Aveti, Anjum M, Ganga Raju M. Antihyperlipidemic activity of methanolic extract of Syzygium alternifolium bark against high-fat diet and dexamethasone induced hyperlipidemia in rats. Asian Journal of Pharmaceutical and Clinical Research. 2015; 8(6): 165-168.
13. Venugopal A and Ramakrishna S. Indirect assessment of hydroxymethylglutaryl-CoA reductase (NADPH) activity in liver. *Clin Chem*. 2005; **21**: pp 1523-1525.
14. Wiesenberg I, Chiesi M, Missbach M, Spanka C and Pignat W. Specific activation of the nuclear receptor PPARγ and RORA by the antidiabetic thiazolidinedione BRL 49653 and the antiarthiritic thiazolidinedione derivative GGP 52608. *Mol Pharmacol*. 1998; **53**: pp 1131-1136.
15. Xu Y, He Z and King GL. Introduction of hyperglycaemia and dyslipidaemia in the pathogenesis of diabetic vascular complications. *Curr Diabetic Rep*. 2005; **5(2)**: pp 91-97.

*This page is intentionally left blank*

# Development of the Quantum Diffusion Model for Impurity H Atoms in Low-Dimensional Nanosystems

*Dr. S. Bobyr*

## ABSTRACT

The quantum diffusion model for impurity atoms in low-dimensional nanosystems has been developed with software for calculating the quantum diffusion coefficients for impurity atoms in materials at different temperatures. The temperature dependence of the quantum diffusion of hydrogen and deuterium on the ice surface is calculated, which shows that it is very close to a straight line in logarithmic coordinates. It has been shown that the quantum diffusion coefficient of hydrogen is about 35 times greater than the diffusion coefficient of deuterium at the temperature of 10 K. The developed model was used to calculate the dependence of the hydrogen quantum diffusion coefficient in a graphone on temperature. It has been established that at temperatures above 200 K, thermally activated diffusion of H begins to dominate, and at temperatures below 150 K, diffusion of hydrogen in graphone occurs by tunneling.

*Keywords:* atom, quantum diffusion, potential barrier, hydrogen, ice surface, graphone.

*Classification:* ACM Codes: G.1.0, G.1.1, G.1.2, G.1.3

*Language:* English

Great Britain Journals Press

LJP Copyright ID: 925611
Print ISSN: 2631-8490
Online ISSN: 2631-8504

London Journal of Research in Science: Natural and Formal

Volume 23 | Issue 10 | Compilation 1.0

# Development of the Quantum Diffusion Model for Impurity H Atoms in Low-Dimensional Nanosystems

Dr. S. Bobyr

## ABSTRACT

*The quantum diffusion model for impurity atoms in low-dimensional nanosystems has been developed with software for calculating the quantum diffusion coefficients for impurity atoms in materials at different temperatures. The temperature dependence of the quantum diffusion of hydrogen and deuterium on the ice surface is calculated, which shows that it is very close to a straight line in logarithmic coordinates. It has been shown that the quantum diffusion coefficient of hydrogen is about 35 times greater than the diffusion coefficient of deuterium at the temperature of 10 K. The developed model was used to calculate the dependence of the hydrogen quantum diffusion coefficient in a graphone on temperature. It has been established that at temperatures above 200 K, thermally activated diffusion of H begins to dominate, and at temperatures below 150 K, diffusion of hydrogen in graphone occurs by tunneling.*

*Keywords:* atom, quantum diffusion, potential barrier, hydrogen, ice surface, graphone.

*Author: KTH Royal Institute of Technology, Brinellvägen 8, SE-100 44, Stockholm, Sweden.*

## I. INTRODUCTION

Hydrogen (H) is the most common element in the Universe, so its diffusion is a very important process in various fields of science, such as astrochemistry [1], materials science and technical sciences [2, 3]. The atoms of H and deuterium (D) exhibit a noticeable wave nature at low temperatures, so their diffusion by tunneling on the surface of solids is given considerable attention [4–11]. Of great importance is the assessment of the parameters of hydrogen diffusion in materials with low dimensionality based on graphene, as possible hydrogen accumulators and elements of modern electronic devices [4–11].

At the same time, the tunneling diffusion of H atoms on water ice is the subject of modern research due to its importance for astronomy and astrochemistry [13-16]. Unlike metal surfaces, H atoms are easily desorbed from water ice at low temperatures below 20 K [14, 16], so studying the migration of H atoms on water ice, as well as the transition from thermally activated to tunneling diffusion, is a difficult task.

It was established in [14] that the surface diffusion of H atoms occurs approximately two orders of magnitude faster than the diffusion of D atoms, which cannot be explained by a classical thermal jump. This experimental evidence of tunneling on the ice surface should be explained by an adequate model of quantum diffusion. Therefore, it is of interest to estimate the parameters of hydrogen quantum diffusion on the ice surface at low temperatures and compare it with thermal diffusion.

In this case, to calculate the parameters of quantum diffusion of hydrogen, it is necessary to apply a suitable quantum mechanical model of atomic tunneling. One of such models for calculating the parameters of quantum diffusion was proposed in [17].

*The purpose of this work:* Is to develop of the proposed model of particle tunneling in low-dimensional nanosystems and its application to estimate the parameters of quantum diffusion of hydrogen and deuterium on the surface of ice and graphone.

## II. THEORETICAL METHOD

To describe the tunneling of an impurity atom through a potential barrier, we use a quantum-mechanical model of a particle with a mass $m_0$ located in a rectangular potential well of width a, bounded on one side by an infinitely high wall (x=0), and on the other (x=l) by a potential barrier height $U_0$ and width $a=l_1-l$. If at some time t<0 the width of the potential barrier is $a\to\infty$, then the particle is localized inside the low-dimensional "space" (0, l) and its wave function inside the potential well has a discrete spectrum $E = E_0$ (Fig. 1) [18].

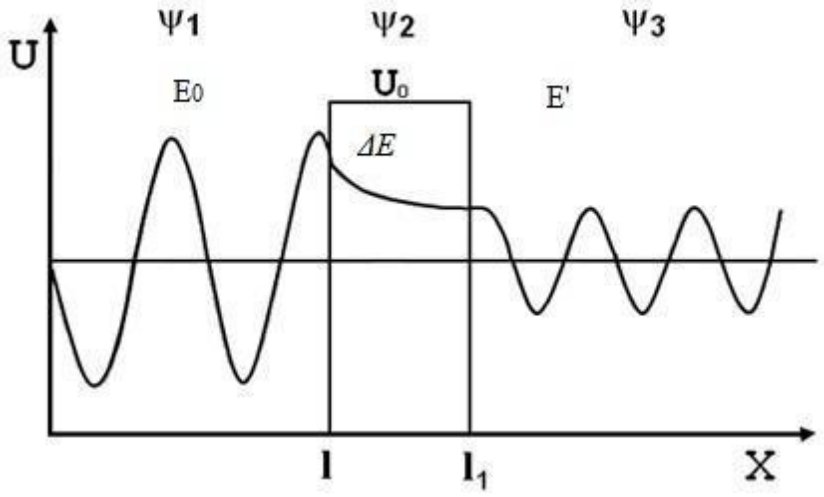


*Figure 1:* Model of quantum diffusion of an atom through a potential barrier

Wave function of a particle at an arbitrary time t≥0 for three regions: 1 ($o<x<l$), 2 ($l<x<l_1$) and 3 ($l_1<x$) are [18]:

$$\Psi_1 = A_1 \sin kx; \quad (1)$$

$$\Psi_2 = A_2 e^{-\eta(x-l)} + B_2 e^{\eta(x-l)}; \quad (2)$$

$$\Psi_3 = A_3 e^{ik(x-l_1)}, \quad (3)$$

where $k^2 = \frac{2m_0}{\hbar^2} E$, $\hbar$ – Planck's constant,

$$\eta^2 = \frac{2m_0}{\hbar^2}(U_0 - E)$$

> 0.

The solution $\Psi_1$ for the first region is chosen in such a way that at x=0 it vanishes, and in the solution in the third region only the wave leaving the barrier is left. This leads to the appearance in the system of a quasi discrete spectrum consisting of quasi levels [18]. From the condition of continuity of the wave function of the particle at the boundaries of the barrier, the docking conditions are found.

At the $x=l$:

$$A_1 \sin kl = A_2 + B_2, \quad (4)$$

$$A_1 \cos kl = (B_2 - A_2)\, k/\eta. \quad (5)$$

At $x = l_1$:

$$A_2 e^{-\eta a} + B_2 e^{\eta a} = A_3, \tag{6}$$

$$A_2 e^{-\eta a} - B_2 e^{\eta a} = -ikA_3/\eta, \tag{7}$$

where $a = l_1 - l$.

The following relations follow from the last two equations:

$$A_2 = \frac{1 - ik/\eta}{2} e^{\eta a} A_3 \tag{8}$$

$$B_2 = \frac{1 + ik/\eta}{2} e^{-\eta a} A_3 \tag{9}$$

From there, using some transformation [17, 18], for the energy $E$ of the particle, we find with accounting the additions:

$$E = \frac{\bar{h}^2 k^2}{2m_0} = \frac{\bar{h}^2}{2m_0}\left[k_0^2 - k'^2 - 2ik' k_0\right] = E' - i\hbar\lambda, \tag{10}$$

is the quasi discrete energy spectrum of the particle,

$$E' = E_o - \Delta E = \frac{\bar{h}^2}{2m_0}\left[k_0^2 - k'^2\right] \tag{11}$$

$E'$ is energy of particle in region 3,

$\Delta E$ – emitted energy passing through the barrier,

$$\lambda = 2v_o k' = D_0 \frac{v_0}{2l} \exp\left[-2a\sqrt{\frac{2m_0}{\bar{h}^2}(U_0 - E_0)}\right], \tag{12}$$

is a damping factor,

$$D_0 \cong \frac{16(k_0/\eta_0)^2}{\left[1 + (k_0/\eta_0)^2\right]^2} \tag{13}$$

is a barrier transparency coefficient,

$v_o = \frac{\bar{h}k_0}{m_0}$ is the particle velocity in region 1.

The presence of the additive $\Delta E$ in the expression for the particle energy (11) means that in the quasi discrete spectrum the particle energy decreases by $\Delta E$ compared to the energy in region 1. This state of the system corresponds to the particle velocity in region 3:

$$v' = . \frac{\bar{h}}{m_0}\sqrt{k^2 - k'^2} \tag{14}$$

Consequently, when passing through the energy barrier, the atom loses speed and, therefore, radiates, reducing its energy by ΔE. The presence of the imaginary part in the expression for energy (11) indicates that the wave function of a particle in a potential well will decrease with time according to an exponential law. In this case, for the square of the modulus of the wave function, we will have:

$$|\psi|^2 = Ae^{-\lambda t} \tag{15}$$

where λ is the so-called damping factor, which characterizes the decrease in the probability of finding a particle inside the potential well.

Thus, the damping coefficients in regions 1 (inside the potential barrier) and 3 (outside the potential barrier) differ by a small amount equal to $v_x = 2\Delta v k'$. This means that the probability of detecting a particle in region 1 changes with time as $|\psi_1|^2 = A_1^2 e^{-\lambda t}$, and the probability of detecting a particle in region 3 as $|\Psi_3|^2 = A_3^2 e^{-\lambda' \tau}$, where $\lambda' = 2v'k'$ is the damping factor for region 3 [17].

Using these expressions, we can make an equality:

$$|\psi_1(\tau)|^2 = |\Psi_3(\tau)|^2 \Rightarrow A_1^2 e^{-\lambda \tau} = A_1^2 e^{-2\eta a} e^{-\lambda' \tau}, \quad (16)$$

And from here find the time τ, after which the amplitudes of the wave functions in regions 1 and 3 will have the same value [17]:

$$\tau = 2\eta a / v_x. \quad (17)$$

Consequently, after a time τ determined by formula (17), the probability of a particle staying in region 3 outside the potential barrier will be equal to the probability of its localization inside the potential well. Therefore, the time τ can also be used as the period the atom is in the potential well.

We can also calculate the time of half-life well-known from the quantum mechanics [18]:

$$\tau_h = 1/(2\lambda) = 1/(4v_0 k') \quad (18)$$

This value of time will be considered calculated according to the basic model.

The calculation of thermally activated diffusion of hydrogen on the ice surface was performed according to the equation of the statistical model proposed in [19]:

$$D = D_o \exp(-U_o/RT), \quad (19)$$

where $D_o = A_o T^2$.

The presented simple model is largely applicable to the description of the quantum diffusion of atoms of elements (hydrogen, nitrogen, carbon) at low temperatures. Software has been developed for calculating the parameters of quantum diffusion of elements in materials at different temperatures.

## III. CALCULATION OF THE PARAMETERS OF QUANTUM DIFFUSION OF HYDROGEN AND DEUTERIUM ON THE ICE SURFACE

As an example of the application of the model, we will consider the diffusion of hydrogen and deuterium on the surface of ice molecules as a two-dimensional system, at low temperatures (Fig. 2). In [20, 21], an experimental design was proposed to study the surface diffusion of H and D atoms on the ice surface, which combines photo stimulated desorption (PSD) and resonantly enhanced multiphoton ionization (REMPI). It is the zero-point energy difference for the jump between H and D atoms that causes the semiclassical kinetic isotope effect (KIE) [20]. Previously, a small KIE was reported in [21] for the diffusion of H and D atoms on the ice surface at 8 K and activation energies are of 22 and 23 meV for the diffusion of H and D atoms, respectively. On the contrary, at higher atomic fluxes, the D/H ratio, especially for polycrystalline ice, increases to ~10 [14]. This large KIE cannot be explained by a thermal jump and is clear evidence of quantum tunneling diffusion of atoms on the ice surface.

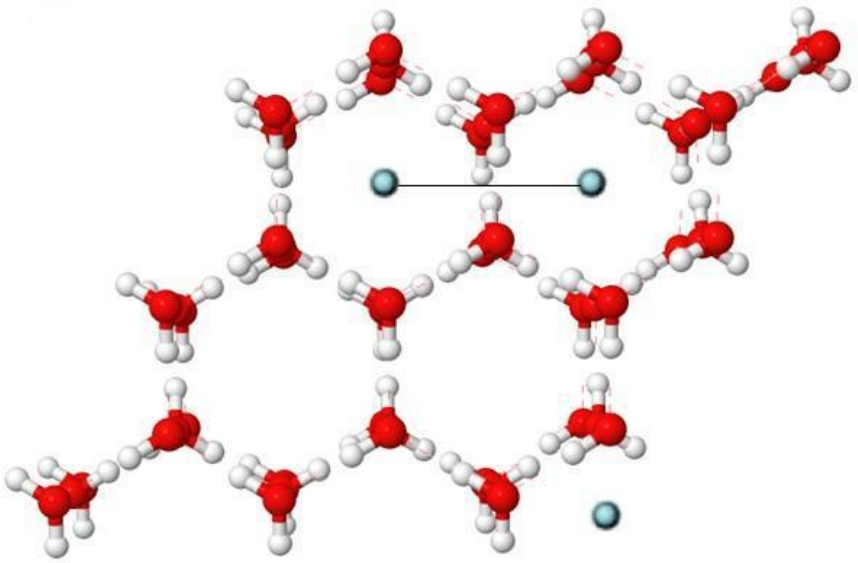

*Figure. 2:* Scheme of diffusion of a delocalized hydrogen atom (deuterium) on the surface of ice molecules. One of 6 equivalent directions of an atom motion is indicated. Oxygen atoms are shown red, valent hydrogen atoms by white and delocalized hydrogen (deuterium) atoms by blue.

Using the parameters given above, we calculate the quantum diffusion coefficient for hydrogen and deuterium atoms located on the ice surface. For calculations, we will use the proposed low-dimensional model and assume that the dimensions of the potential well l and potential barrier a are equal to half the period *d* of the ice crystal lattice (0.225 nm). Considering 6 equivalent directions of motion of the hydrogen atom (and deuterium) on the ice surface, the diffusion coefficient will be calculated by the formula:

$$D = d^2/6\tau, \qquad (20)$$

where τ is the time spent by the particle in the potential well, determined by the basic equation (18) and equation (17) of the proposed model. For comparison, the over-barrier diffusion coefficient was also calculated, and the results are presented in Fig. 3.

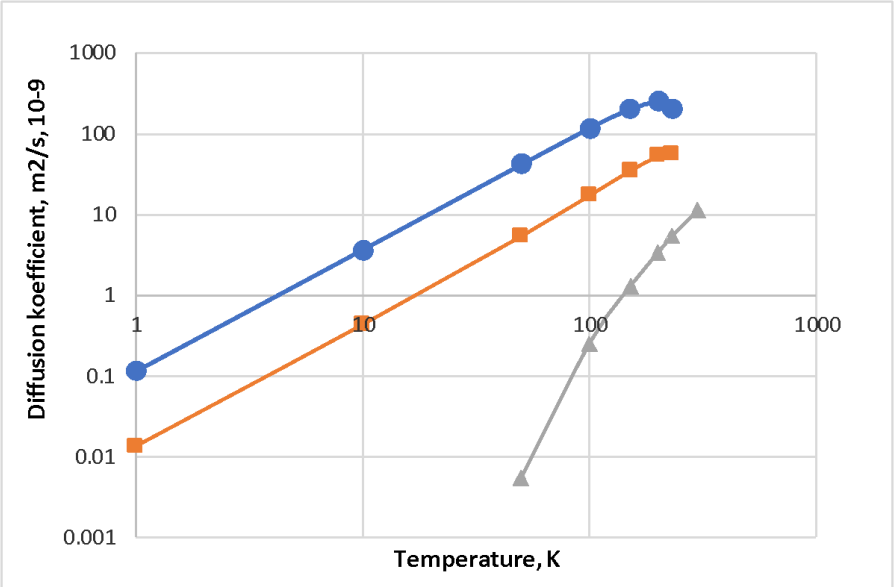


a

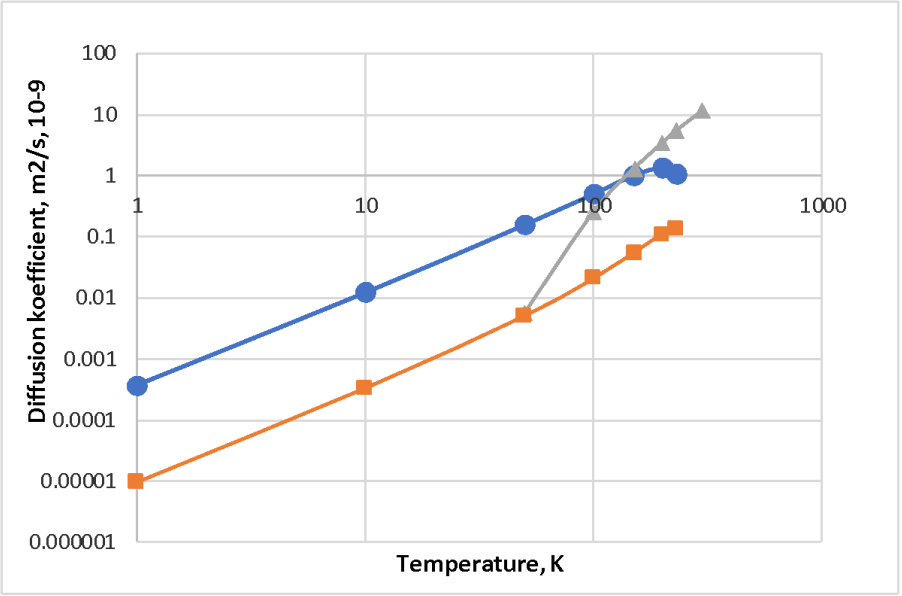


b

*Figure 3:* Quantum diffusion H (blue line with balls) and Deuterium (orange line with squares) on the surface of ice, with the estimate of over barrier diffusion H (gray line with triangles), a in the basic model, b in the developed model.

Based on the above results, the following conclusions can be drawn. The calculation of the time spent by a particle in a potential well using the basic formula (18) gives underestimated values of the time spent by a particle in a potential well and high values of the diffusion coefficient (Fig. 3a). The values of the quantum diffusion coefficients, calculated by equation (18), significantly exceed the value of the thermal diffusion coefficient in the entire range of temperatures under consideration.

The proposed simple model makes it possible to obtain quite acceptable refined, in comparison with [17], values of these parameters at T=10 K, namely $D_H = 1.21 \cdot 10^{-11}$ $m^2/s$ and $D_D = 3.37 \cdot 10^{-13}$ $m^2/s$. The quantum diffusion coefficient of hydrogen is about 35 times greater than the diffusion coefficient of deuterium at this temperature. This result was previously obtained theoretically in [17], allowing us to satisfactorily explain the experimental data of [14]. In the basic model, this ratio is about 8 and does not allow explaining the observed experimental ratio.

In the present work, it is established that the quantum diffusion coefficients of hydrogen and deuterium, as well as other elements, depend on temperature. This dependence takes place both in the basic calculation model (Fig. 3a) and in the proposed model (Fig. 3b). Therefore, the dependence of the diffusion coefficients of hydrogen and deuterium on temperature in the range of 10–80 K observed in [14] can be explained precisely by quantum rather than ordinary diffusion through the barrier. This dependence on temperature for hydrogen is very close to a straight line in the Log (D) – Log (T) coordinates.

According to our estimate (Fig. 3b), ordinary hydrogen diffusion becomes more significant than quantum diffusion at temperatures above 150 K. At temperatures below 100 K, thermal diffusion does not contribute to the quantum diffusion of hydrogen and the temperature dependence in the logarithmic coordinates is close to a straight line. This new theoretical result may well be confirmed experimentally.

## IV. CALCULATION OF THE PARAMETERS OF QUANTUM DIFFUSION OF HYDROGEN ON THE GRAPHONE

A promising area of science and technology is the possible use of low-dimensional graphene-based materials for carbon electronics, chemical sensors with extraordinary sensitivity, and hydrogen storage [22].

In [23, 24], the properties of a stable graphone are studied (Fig. 4).

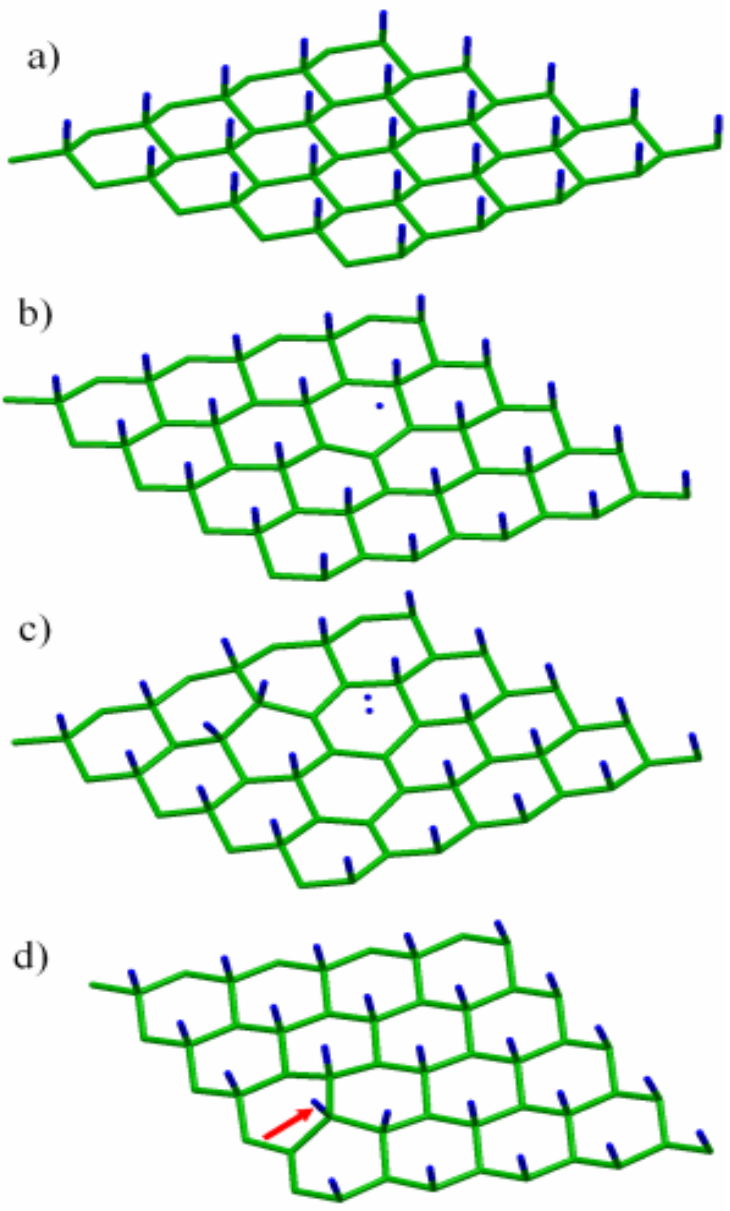


*Figure 4:* Structure of graphone [24]. Optimized atomic structure of pristine graphone (a), graphone with removed one (b) and two (c) adatoms; final step of the migration of adatom (shown by arrow) from one sublattice to another (d). Carbon atoms are shown by green, hydrogen by blue.

Using DFT, Bukhvalov argues that while the energy barrier to hydrogen removal is high enough to make graphone stable, hydrogen atom migration is favorable with an energy barrier of around 0.06 eV, so graphone may not be suitable for use in electronic devices and storage media [24].

Thus, the study of hydrogen diffusion in low-dimensional materials at low temperatures is an important task.

In the present study, we calculate the parameters of quantum diffusion of a delocalized hydrogen atom on the surface of a graphone with an energy barrier of 0.06 eV [24] and a lattice period of 0.246 nm [25].

In accordance with the general provisions of the quantum model, tunneling occurs when the energy of the atom is less than the energy barrier, in this case 0.06 eV, i.e. up to a temperature of about 650 K. However, at a sufficiently high temperature, thermally activated diffusion of atoms through the barrier will also occur. Diffusion coefficients calculated by different models using equations (17) – (20) are shown in Fig. 5.

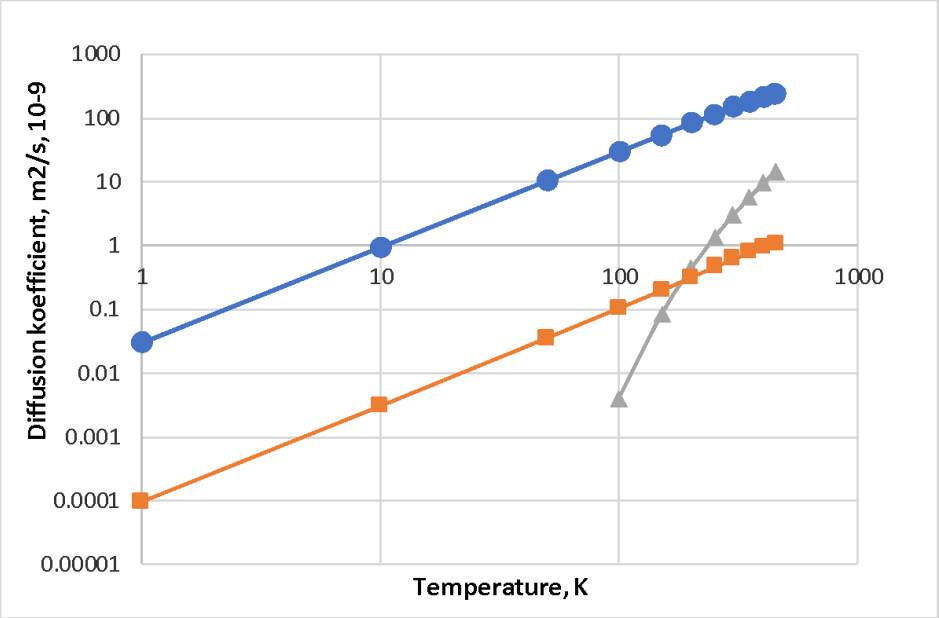


*Figure 5:* Quantum diffusion H in the graphone, with the estimate of over barrier diffusion H (gray line with triangles), blue line with balls – basic model, red line with squares – developed model.

As expected, the basic calculation model overestimated the quantum diffusion coefficient of hydrogen in graphone, exceeding its thermal diffusion coefficient over the entire temperature range.

The proposed model made it possible to obtain an almost linear dependence of the quantum diffusion coefficient of hydrogen in a graphone in the Log (D) – Log (T) coordinates, i.e. there is a dependence (from 1 to 150 K):

$$D_Q(H) = A \times T^N, \, m^2/s \qquad (21)$$

Where $A = 0.977 \times 10^{-13}$ and $N = 1.52$ are the parameters of the developed model. With a small error, we can use a simple equation to calculate the quantum diffusion H in graphone:

$$D_Q(H) = 1.0 \cdot 10^{-13} \times T^{3/2}, \, m^2/s \qquad (22)$$

As shown in fig. 5, thermally activated diffusion of H begins to dominate at temperatures above 200 K, but even at 500 K the contribution of quantum diffusion is approximately 1/10 of the total diffusion. At temperatures below 150 K, hydrogen diffusion in graphone occurs by tunneling in accordance with the proposed dependence (21).

Note that the above model of quantum diffusion does not consider the ZPE -zero-point energy, which significantly affects the tunneling parameters and near the temperature T=0, $D_{Qo}(H) = const$ [14].

## V. CONCLUSIONS

1. A simple quantum mechanical model of atom tunneling through a potential barrier is developed in this work. Software has been developed for calculating the parameters of quantum diffusion of elements in materials at different temperatures.
2. The temperature dependence of the quantum diffusion of hydrogen and deuterium on the ice surface is calculated. The values of the quantum diffusion coefficients are obtained at T=10 K, $D_H = 1.21 \cdot 10^{-11}$ $m^2/s$ and $D_D = 3.37 \cdot 10^{-13}$ $m^2/s$, respectively. The quantum diffusion coefficient of hydrogen is about 35 times greater than the diffusion coefficient of deuterium at this temperature, allowing a satisfactory explanation of the experimental results.
3. In the present work, it is established that the quantum diffusion coefficients of hydrogen and deuterium, as well as other elements, depend on temperature. This dependence on temperature is very close to a straight line in the logarithmic coordinates. The experimentally observed dependence of the diffusion coefficients of hydrogen and deuterium on temperature in the range of 10–80 K can therefore be explained precisely by quantum rather than ordinary diffusion through the barrier. It is shown that thermally activated diffusion does not affect the diffusion of hydrogen at these temperatures.
4. The developed model is used to calculate the quantum diffusion coefficients of hydrogen in a low-dimensional material - graphone with an energy barrier of 0.06 eV. Theoretically, the dependence of the values of the coefficient of quantum diffusion of hydrogen in graphone on temperature is established in the form $D_Q(H) = A \times T^N$.
5. It has been established that the thermally activated diffusion of H in graphone begins to dominate at temperatures above 200 K, but even at a temperature of 500 K the contribution of quantum diffusion is 1/10 of the total diffusion. At temperatures below 150 K hydrogen diffusion in graphone occurs by tunneling.

## REFERENCES


1. V. K. Veeraghattam, K. Manrodt, S. P. Lewis, and P. C. Stancil, Astrophys. J. 790, 4 (2014).
2. Pozzo, M., Alfe, D. Hydrogen dissociation and diffusion on transition metal (= Ti, Zr, V, Fe, Ru, Co, Rh, Ni, Pd, Cu, Ag)-doped Mg (0001) surfaces. Int. J. Hydrogen Energy, 2009, 34,1922-1930. DOI: 10.1016/j.ijhydene.2008.11.109.
3. Li, X., Ma, X., Zhang, J., Akiyama, E., Wang, Y., Song, X. Review of Hydrogen Embrittlement in Metals: Hydrogen Diffusion, Hydrogen Characterization, Hydrogen Embrittlement Mechanism and Prevention. Acta Metall. Sinica (English Letters), 2020, 33, 759-773. https://doi.org/10.1007/s40195-020-01039-7/.
4. McIntosh, E. M.; Wikfeldt, K. T.; Ellis, J.; Michaelides, A.; Allison, W. Quantum effects in the diffusion of hydrogen on Ru (0001). J. Phys. Chem. Lett., 2013, 4, 1565–1569, DOI: 10.1021/jz400622v.
5. Jewell, A. D., Peng, G., Mattera, M. F. G., Lewis, E. A., Murphy, C. J., Kyriakou, G., Mavrikakis, M., Sykes, E. C. H. Quantum tunneling enabled self-assembly of hydrogen atoms on Cu (111) ACSNano, 2012, 6, 10115– 10121, DOI: 10.1021/nn3038463.
6. Fang, W., Richardson, J.O., Chen, J., Li, X.-Z., Michaelides, A. Simultaneous deep tunneling and classical hopping for hydrogen diffusion on metals. Phys. Rev. Lett., 2017, 119, 126001, DOI: 10.1103/PhysRevLett.119.126001.
7. Sundell, P. G., Wahnström, G. Activation Energies for Quantum Diffusion of Hydrogen in Metals and on Metal Surfaces using Delocalized Nuclei within the Density-Functional Theory. Phys. Rev. Lett., 2004, 92, 155901, DOI: 10.1103/PhysRevLett.92.155901.
8. Vykhodets, V., Nefedova, O., Kurennykh, T., Obukhov, S., Vykhodets, Y. Quantum Diffusion of Deuterium in Sodium. J. Phys. Chem. A 2019, 123, 7536– 7539, DOI: 10.1021/acs.jpca.9b06231.

9. S. Cazaux and a. G. G. M. Tielens, Astrophys. J. 715, 698 (2010).
10. W. Iqbal, K. Acharyya, and E. Herbst, Astrophys. J. 751, 58 (2012).
11. L. Reboussin, V. Wakelam, S. Guilloteau, and F. Hersant, Mon. Not. R. Astron. Soc. 440, 3557 (2014).
12. R. Gomer, Rep. Prog. Phys. 53, 917 (1990).
13. L. J. Lauhon and W. Ho, Phys. Rev. Lett. 85, 4566 (2000).
14. K. Kuwahata, T. Hama, A. Kouchi, and N. Watanabe. Signatures of Quan-tum-Tunneling Diffusion of Hydrogen Atoms on Water Ice at 10 K. Phys. Rev. Lett. 115, 133201 (2015).
15. C. Z. Zheng, C. K. Yeung, M. M. T. Loy, and X. Xiao, Phys. Rev. Lett. 97, 166101 (2006).
16. T. Hama and N. Watanabe, Chem. Rev. 113, 8783 (2013).
17. S.V. Bobyr. Development and Application of a Simple Model for Calculation the Quantum Diffusion Parameters of Rubidium, Hydrogen and Deuterium Atoms. Scientific Herald of Uzhhorod University, Series Physics, 2021, V.49, P.19-25. DOI:10.24144/ 245-8038.2021.49.19-25.
18. A.A. Sokolov, I.M. Ternov, V.Ch. Zhukovsky, Quantum Mechanics [in Russian]. Nauka, Moscow. (1979), 528 p.
19. S.V. Bobyr. Statistical model of impurity atoms diffusion in the crystal lattice of metals and its application for calculating the diffusion coefficients of hydrogen and carbon atoms in iron. Semiconductors or Physics of the Solid State 3, 345 (2021).
20. N. Watanabe, Y. Kimura, A. Kouchi, T. Chigai, T. Hama, and V. Pirronello, Astrophys. J. 714, L233 (2010).
21. T. Hama, K. Kuwahata, N. Watanabe, A. Kouchi, Y. Kimura, T. Chigai, and V. Pirronello, Astrophys. J. 757, 185 (2012).
22. Peng Q., Dearden A. K., Crean J., Han L., Liu S., Wen X., De S. New materials graphyne, graphdiyne, graphone, and graphane: review of properties, synthesis, and application in nanotechnology. Nanotechnol. Sci. Appl., 2014, 7, 1–29. (doi:10.2147/NSA. S40324).
23. Boukhvalov D.W., Katsnelson M.I., Lichtenstein A.I. Hydrogen on graphene: electronic structure, total energy, structural distortions and magnetism from first-principles calculations. Phys. Rev. B., 2008, 77, 035427. DOI: https: //doi.org/10.1103/PhysRevB.77.035427.
24. Boukhvalov D. W. Stable antiferromagnetic graphone. Physica E. 2010; 43:199–201.
25. Katsnelson M. I. Graphene: Carbon in Two Dimensions. — New York: Cambridge University Press, 2012. — 366 p. - ISBN 978-0-521-19540-9.

# Short and Long Term Effects of Water Markets

*Rim Lahmandi-Ayed & Mohamed Salah Matoussiy*

*Université de Tunis*

## ABSTRACT

We aim at checking from a theoretical viewpoint the claims made about water markets in the literature. We prove that water markets improve farmers' profits and production eficiency but do not necessarily improve total production and do not always encourage private investments. Taking into account the transaction cost of water markets and the social cost due to the inactivity of some farmers that may result from water markets, we prove that water markets do not always improve total surplus

*Keywords and phrases:* water markets, water scarcity, production e_ciency, total production, private investment, social costs, transaction costs.

*Classification:* UDC Codes: 338.4791, 338.477, 338.47

*Language:* English

Great Britain Journals Press

LJP Copyright ID: 925612
Print ISSN: 2631-8490
Online ISSN: 2631-8504

London Journal of Research in Science: Natural and Formal

Volume 23 | Issue 10 | Compilation 1.0

# Short and Long Term Effects of Water Markets

Rim Lahmandi-Ayed[α] & Mohamed Salah Matoussiy[σ]

## ABSTRACT

*We aim at checking from a theoretical viewpoint the claims made about water markets in the literature. We prove that water markets improve farmers' profits and production eficiency but do not necessarily improve total production and do not always encourage private investments. Taking into account the transaction cost of water markets and the social cost due to the inactivity of some farmers that may result from water markets, we prove that water markets do not always improve total surplus.*

*Keywords and phrases:* water markets, water scarcity, production effciency, total production, private investment, social costs, transaction costs.

*Author:* UR. MASE-Ecole Sup_erieure de la Statistique et de l'Analyse de l'Information, Université de Carthage, Université de Tunis.

## I. INTRODUCTION

In several countries having limited water resources, water is being sold cheaply, which encourages water wasting behaviour. The design of an adequate pricing to urge users to take water scarcity into account, implying necessarily a substantial rise of prices, would probably meet resistance from users and would moreover require accurate information on demands. Water markets have been precisely suggested to manage more efficiently water resources while ensuring traditional users' approval, without requiring information on demands. Each user is given a water use right on the basis of his/her historical use at the historical price. An exchange of these rights is allowed, which should lead to a new water price better revealing the water value as it results from a balance of water offer and demand. It should be expected that water markets would result in a more efficient use of water, an improvement of farmers' situation, an improvement of total production thus in an improvement of social welfare. In this paper, we aim to check whether these expectations are always theoretically founded, taking into account the transaction cost of water markets and the social cost due to the inactivity of some farmers that may result from water markets.

In several countries and regions around the world, although water provision requires high costs, water is being attributed through quotas to farmers at very low prices. Some farmers are using water inefficiently (with regard to its real value) while other more efficient farmers are not being satisfied with the quantities received. A water market would result in a balance between offer and demand, thus avoiding the rationing of farmers, and in water transfer from the least to the most efficient farmers (Lahmandi-Ayed and Matoussi, 2003). When the efficiency difference between farmers is sufficiently high, some farmers among the most inefficient ones would stop production activity. This very advantage in terms of water use may have highly negative socio-

London Journal of Research in Science: Natural and Formal

economic impacts. First inefficient farmers becoming inactive, are very likely to move to cities with all the related families thus increase the number of rural exoders with all their urban, social, political and economic problems mainly in the developing countries. Second they are unemployed persons. The possibility of conversion to another activity is only theoretical for the major part of farmers who are poorly educated thus hardly convertible. Third from the viewpoint of junior farmers, the introduction of a water market results in the introduction of an intermediary in water sale, thus in a rise of water prices. Within a short period, junior farmers will become themselves "senior", and may dislike that a difference remain, which may result in a tenseness in farmers' relationship. Finally people may not think acceptable that a resource involving high public costs, be offered graciously to inefficient farmers that will live on its sale or rent. Hence there is a real cost to put some farmers outside the productive sector which is taken simply into account in this paper.

In the long run water markets are expected to urge farmers to invest in water saving technologies to sell the water saved, which would mitigate at least some of the short term drawbacks. The few empirical observations on the question are contradictory. According to Hearne and Easter (1995), concerning the Chilean water market experience, farmers sell in general a part of their use rights, which allows them to invest in new irrigation techniques that conserve better the resource and results in improving the global production without requiring new mobilizations harmful to the environment. However, according to Bauer (1997) concerning the same experience, "despite expectations on the contrary, there has been almost no private investment in irrigation technology for the purpose of selling rights to the water saved". In Most of Chile, the author observes that water use efficiency remains at its traditional level and that flood irrigation remains the dominant practice. Therefore the question of whether water markets foster private investments in water saving technologies, needs to be explored from a theoretical viewpoint.

We consider a simple model involving unequally efficient farmers. We suppose that water resources are being rationed. In the short run farmers have only the possibility of exchanging water. We prove that in the short run water markets improve farmers' profits thus production efficiency but do not necessarily improve total production. Taking into account the transaction cost of water markets and the social cost due to the inactivity of some farmers which may result from water markets, we prove that water markets do not necessarily improve social welfare. In the long run farmers have the possibility of investing in water saving technologies before exchanging water rights. We prove that water markets do not always foster private investments when compared to the status quo (situation without water market).

*The related literature.* Water markets look very similar to tradeable pollution permits. Thus it would be natural to compare our results concerning the investment decisions of farmers in the long run with the papers dealing with the innovation in pollution abating technologies within polluting industries, even if a main difference

exists compelling to deal separately with each sort of problem: a pollution permit is not an input as it is the case for water rights. Malueg (1989) and Milliman and Prince (1989) prove that the introduction of tradeable pollution permits may actually decrease some firms' incentives to adopt more effective pollution control technologies. But both papers examine the question at the firm's level. Jung, Krutilla and Boyd (1996) extend Milliman and Prince's approach from the firm to the industry level. They prove that auctioned permits provide the most incentive effects to promote the development and adoption of advanced pollution abatement technology. But Jung et al. model the pollution permits price mechanism only roughly while in our model the water price is function of the investment decisions since the demand of each farmer is function of his/her level of investment. The more recent paper of Requate (1998) examines the incentives to innovate (adopt a cleaner technology) within a polluting industry under emission taxes and tradeable permits. Requate proves that "there is no unique ranking between those tools, i.e. neither does one of the two tools provide a higher incentive to adopt a new technology in all cases". His conclusion is close in spirit to our own one in that tradeable rights do not necessarily provide higher incentives to innovate. His model is richer than the previous ones in that he models more richly the pollution price mechanism and takes the feedback on the ouput market into account. The weakness of the previous paper lies nevertheless in the hypothesis that only one firm has the possibility of adopting the new cleaner technology, while the possibility of investing in water saving technologies is given in our paper to all inefficient farmers.

The paper is organized as follows. Section 2 describes the model. Section 3 deals with the short term effects of water markets. Section 4 deals with their long term effects mainly in terms of private investment. Section 5 concludes. An appendix contains the proofs.

## II. THE MODEL

### *2.1 The general framework*

Consider $n$ farmers $(i = 1, .., n)$ producing a homogenous farm good sold at an exogenous price $p$. This is a simplifying but reasonable hypothesis as a water market is local while the output trade may be made at a national or international level. The model accounts for the effect of a local switch to water market within a given group of farmers sharing a given water resource, which thus has a negligible effect on the output price.

The limiting factor is supposed to be water thus the produced quantity and costs may be expressed function of the quantity of water used. More precisely, when the quantity of water $x_i$ is applied by farmer $i$, $f_i(x_i)$ is the quantity of farm good produced, while $C_i(x_i)$ is the total cost stemming from inputs other than water (fertilizers, labor, chemicals...). Functions $f_i$ and $C_i$ are naturally supposed to be increasing. We suppose that they are twice continuously differentiable with $\frac{\partial^2 f_i}{\partial x_i^2} \leq 0$ hence $f_i$ is concave, while $\frac{\partial^2 C_i}{\partial x_i^2} \geq 0$ hence $C_i$ is convex, and that at least one among the two inequalities is strict.

Denote by $\Omega$ the total exogenous offer. The authority assigns a given quota $\omega_i$ to each farmer $i$. We have $\Omega = \sum_{i=1}^{n} \omega_i$.

We refer to *status quo* the situation without water market. In this situation, each farmer may buy a quantity of water up to his/her quota $\omega_i$, at the historical price $p_h = 0$. Hypothesis $p_h = 0$ supposed for simplicity is close to reality in several developing countries as Tunisia or Egypt for instance. Farmer $i$'s profit in the status quo is given by:

$$\pi_i(x_i) = pf_i(x_i) - C_i(x_i).$$

The solution of the first order condition $\pi_i'(x_i) = pf_i'(x_i) - C_i'(x_i) = 0$ is denoted by $\tilde{x}_i^s$. The demand of farmer $i$ if he/she were not constrained by his/her quota is: $x_i^s = \max(\tilde{x}_i^s, 0)$.

Taking farmer $i$'s quota into account, his/her actual demand $d_i^s$ is given by:

$$d_i^s = \begin{cases} x_i^s & \text{if} \quad x_i^s < \omega_i \\ \\ \omega_i & \text{if} \quad x_i^s \geq \omega_i \end{cases}$$

We suppose that

$$\sum_{i=1}^{n} x_i^s > \Omega. \tag{1}$$

This inequality means that the total desired quantity is not satisfied, which would be natural in a scarcity context. It will also ensure as we will see the existence of a price equilibrium when a water market is introduced. This implies that there exists necessarily some rationed farmers, i.e. such that $x_i^s > \omega_i$.

In the welfare analysis, we focus on the implied group of farmers and the authority who organizes the water market (who is inactive in the status quo). This partial analysis is a first step to have an idea on the effect of water markets on the agricultural sector taking into account their direct costs. The explicit consideration of interests outside the group of farmers and the organizing authority would require at least to model adequately the output market thus for instance to deal with water market within the other groups of farmers and to have information on the demand side. This would be a more complete treatment of the subject and may be a further step of the present research. However the demand side is implicitly dealt with through the examination of the effect of water market on total production.

The social welfare in the status quo is given by

$$W_s = \sum_{i=1}^{n} \pi_i(d_i).$$

Suppose now that a water market is introduced. We suppose that this involves a transaction cost $T$, often mentioned in the literature. The transaction cost $T$ is a global cost corresponding to all the costs incurred by the organizing authority to set up the water market and make it work. In this paper, we suppose that farmers do not pay fees to the organizing authority when they participate in the water market. Cost $T$ thus corresponds someway to a cost assumed by the remaining of the society

in order to promote water markets. Indeed when a new practice is introduced, even if it is expected to do only good, the mere mentioning of a fee to be paid may give rise to suspicion thus may discourage the adhesion of farmers. Thus we think that the transaction cost should be incurred entirely by the organizing authority at least for some period of time if it wants to promote water markets. If farmers were to pay fees, the sharing of the transaction cost is not a simple issue and the conclusions of the paper may change substantially depending on the way those fees are calculated, another issue which can be dealt with in a next work.

Section 3 deals with the short term effects of water markets. Farmers have only the possibility after receiving their quotas to exchange water, which results in a new price $p_e$. We suppose that they are price-takers.

Under some conditions water markets result in the inactivity of some farmers. We suppose that this inactivity involves a social fixed cost $S$ per each inactive farmer. Cost $S$ may be viewed as the cost necessary to solve all the problems implied by the inactivity of one farmer (rural exodus, conversion to another activity...)[1].

### 2.2 A specification of the model for the long run

Section 4 deals with the long term effects of a water market. We suppose that in the long run farmers have the possibility of making investments to "improve their productivities" before water exchange. To deal simply with the long run, we choose a particular specification of the relevant functions.

We suppose that all farmers produce with the same cost function $C_i(x_i) = cx_i^2$ and that the $n$ farmers are divided into two homogeneous groups. The first group involves $q$ "inefficient farmers" ($q \geq 2$), $i = 1, \cdots, q$, i.e. that have the same function $f_1(x) = \delta_1 x$, thus the same low "productivity" $\delta_1$. The second group involves $m$ "efficient farmers", $i = q+1, \cdots, q+m$, "up-to-date" i.e. that have the best possible productivity $\delta_2$, implying function $f_2(x) = \delta_2 x$. Parameters $\delta_1$ and $\delta_2$ correspond to the quantity of ouput obtained per unit of water used, respectively by inefficient and efficient farmers. The unit of the farm good is chosen such that $\delta_2 = 1$.

In order to check whether the long term effects of water markets mitigate the short term ones, the difference between the two productivities is chosen such that only the efficient farmers would remain productive in the short run if a water exchange were to take place[2]. For simplicity, we consider a specific numerical case: $\frac{c\Omega}{mp} = 1/4$ and $\delta_1 = 1/3$; and we take the case of farmers having the same quota: $\omega_i = \omega$. Hence, the relation $\frac{c\Omega}{mp} = 1/4$ becomes

$$\frac{c\omega}{p} = \frac{m}{4(m+q)}. \tag{2}$$

[1]See the introduction for a more detailed explanation.

In the long run the inefficient farmers have the possibility of improving their productivities. To move from productivity $\delta_1$ to some productivity $\mu$ with $\delta_1 \leq \mu \leq 1$, an inefficient farmer must invest $I(\mu) = a(\mu - \delta_1)$. Parameter $a > 0$ may be called the intensity of investment and measures how intensive an investment must be to move from the initial productivity to some given new one. We suppose that efficient farmers cannot improve their productivites, they have the best available one.

Inefficient farmers are involved in a non-cooperative game in which they choose simultaneously their investment levels (or equivalently the level of their new productivities). In the second step or the "exchange" step, after observing the choices of the first step, with the new productivities, a water exchange occurs between farmers, supposing that farmers have a competitive behaviour.

## III. THE SHORT RUN

In this section we compare the status quo with a water market in the short run from the following viewpoints: the profit of each farmer and production efficiency, total production and social welfare. We prove that a water market always improves each farmer's profit thus production efficiency but does not necessarily improve total production and social welfare.

When a water market is introduced, the profit of farmer $i$ is given by:

$$\pi_i = p_e(\omega_i - x_i) + pf_i(x_i) - C_i(x_i).$$

$p_e(\omega_i - x_i)$ is the part of the profit coming from the exchange (to be further referred to as "exchange profit") which may be either positive if the farmer is globally a water seller or negative if the farmer is globally a water buyer; while $pf_i(x_i) - C_i(x_i)$ is the profit coming from production (to be referred to as "production profit").

Denote by $x_i(p_e)$ the solution of the first order condition:

$$pf_i'(x_i) - C_i'(x_i) = p_e.$$

The demand of farmer $i$ is given by $d_i(p_e) = \max(x_i(p_e), 0)$.
A price equilibrium $p_e^*$ satisfies:

$$\sum_{i=1}^{n} d_i(p_e^*) = \Omega.$$

**Result 1 (Existence of price equilibrium)** *Under the general framework of the model, there exists a unique price equilibrium.*

[2]This is a consequence of a result obtained by Lahmandi-Ayed and Matoussi (2003) recalled in Proposition 1 later in this paper.

Result 1 is needed to ensure that the demonstrated properties have cases of application. It holds for general specifications of $f_i$ and $C_i$ under the general hypotheses supposed in the model.

**Result 2 (Profits, Production efficiency)** *Under the general framework of the model, the water market improves each farmer's profit thus improves production efficiency*

Result 2 is a natural one for, with a water market each farmer has the possibility of applying exactly quantity $d_i^s$ (his/her demand in the status quo), which gives him/her a production profit equal to his/her profit in the status quo, and selling the difference $\omega_i - d_i^s$ at price $p_e$, which gives him/her an additional exchange profit. Water markets offer indeed more possibilities to farmers by releasing the constraint on demands, which necessarily improves the situation of each one of them. Consequently, if they are given the choice, farmers have always interest to participate in the water market.

Denote by $A$ the difference between the sum of profits with a water market at price equilibrium and the sum of profits in the status quo. Necessarily $A > 0$. Hence in terms of production, a water market improves production efficiency in the sense that it improves the profit of the whole sector as it improves each farmer's profit.

However the improvement of production efficiency is not synonymous of the improvement of total production. This is illustrated through the following simple example.

**Result 3 (Total production)** *Suppose that there are two farmers $i = 1, 2$. Farmer $i$ has function $f_i(x_i) = \delta_i x_i$, the cost function $C_i(x_i) = c_i x_i^2$ and the quota $\omega_i = \Omega/2$. Let $\delta_1 = 1$, $\delta_2 = 3$, $c_1 = 0.5$, $c_2 = 2.9$ and $\frac{\Omega}{p} = 1$. With these values of the parameters, the switch to water market decreases total production relative to the status quo.*

Note that we consider the case of two farmers for exposition simplicity. But the same type of result may be proved for two groups of homogenous farmers. The reason that total production decreases with the chosen example is that the most productive farmer has also the highest cost. Thus there is a shift to more production by the farmer with lowest productivity and lowest cost[3]. Obviously the result is not a general one[4] but is provided only to say that it is a possible case. As cost $C_i$ corresponds to the costs implied by the inputs other than water (labor, fertilizers...), the quantities to be used with a given amount of water thus the implied cost $C_i$ may depend on several parameters as the land's slope or the soil's nature. Thus all combinations are *a priori* possible (high productivity with high costs, low productivity with low costs, high productivity with low costs...) including the given example.

Although a water market always increases the profit of each farmer thus always increases total profit (which is true in particular with the chosen example), this does in no way imply an increase of total production. In short terms, the example provided by Result 3 together with the general Result 2 show that the sector may end up earning more and producing less after setting up a water market!

[3]An anonymous referee is thanked for this remark.







London Journal of Research in Science: Natural and Formal

Finally, in terms of welfare, if only the welfare of incumbent farmers is considered, it is obvious that a water market improves the social surplus, since it improves the profit of each one of them. But if the transaction and the inactivity costs are considered, a water market has an ambiguous effect on social surplus.

If equilibrium involves $h$ inactive farmers, the surplus difference between both situations

$$W_w - W_s = A - hS - T.$$

The water market improves the social welfare only if:

$$A - hS - T > 0$$

The last inequality allows to see simply the advantages and disadvantages of water markets, as far as only farmers and the organizing authority are concerned. A water market improves the farmers' profit but involves costs and may result in the inactivity of some farmers. A net benefit would result only if the gain outweighs the losses.

But number $h$ is endogenous. The consideration of a specific example allows to calculate that number and derive conclusions on whether a water market improves welfare, depending on exogenous parameters.

### *An example*

Lahmandi-Ayed and Matoussi (2003) studied the case of linear functions $f_i(x_i) = \mu_i x_i$, $\mu_i$ being the productivity of farmer $i$, and a quadratic cost function $C(x_i) = cx_i^2$. Farmers are supposed to have the same cost function and to differ only by their functions $f_i$. Thus a farmer with a higher productivity is more efficient than a farmer with a lower productivity. Suppose that farmers are ordered as follows: $\mu_1 \leq \mu_2 \cdots \leq \mu_n$. And denote by $(u_i)_{1\leq i\leq n}$ defined by:

$$u_i = \sum_{j=i+1}^{j=n} (\mu_j - \mu_i)$$

At equilibrium "Productive" farmers are those who produce a positive quantity of the farm good and "non-productive" farmers those who make profit only from water resale. Lahmandi-Ayed and Matoussi (2003) proved Proposition 1 stated below.

**Proposition 1 (Lahmandi-Ayed and Matoussi, 2003)** *At the competitive equilibrium,*

1) *if $2c\Omega/p > u_1$ then all the farmers are productive (thus $h = 0$).*
2) *if $2c\Omega/p \leq u_{n-1}$, then only Farmer $n$, the most efficient one, is productive (thus $h = n - 1$).*
3) *otherwise, there exists some integer $2 \leq i \leq n - 1$ such that $u_i < 2c\Omega/p \leq u_{i-1}$, in which case only farmers $j = i, \cdots, n$ are productive (thus $h = i - 1$).*

[4]In the example provided in Proposition 1 a water market increases total production.

What is particular here is that the water market improves not only production efficiency as we defined it, but total production, as water is transferred from the least to the most efficient farmers in terms of production. Moreover in the first case where the difference in productivities is small enough, all farmers remain active.

Consider now *the specification of the model adopted for the long run* which is a particular case of the above one. The parameters of the example have been chosen such that only the efficient farmers are active in the short run if a water market is set up (thus $h = q$).

After calculations, the improvement of the sum of profits due to the water market is equal to $A = (5/12)\frac{qp\Omega}{m+q}$. The water market improves the social welfare only if[5]:

$$(5/12)\frac{qp\Omega}{m+q} - T - qS > 0. \tag{4}$$

Denote by $\alpha = (5/12)p\Omega$. Inequation 4 is equivalent to

$$q < \hat{q} = \frac{\alpha - T - mS + [(\alpha - T - mS)^2 + 4STm]^{1/2}}{2S},$$

which may also be written as:

$$S < \frac{1}{q}[(5/12)\frac{qp\Omega}{m+q} - T].$$

Therefore there is an overall benefit in the short run from a water market only if inefficient farmers are not too numerous and/or the cost due to inactivity of a farmer is not too high. Otherwise, the social welfare worsens with a water market relative to the status quo. Indeed in the opposite case, the improvement of the farmers' profit implied by a water market is not enough to outweigh the too high social costs due to those inactive farmers.

## IV. THE LONG RUN

We now suppose that farmers have the possibility of investing in water saving technologies as in the specification described in the model for the long run. As in the short run case, it is easy to check that a water market improves each farmer's profit thus production efficiency. Hence each farmer has interest to participate in the water market if he/she is given the choice. However we prove that a water market does not always encourage private investments relative to the status quo.

**Result 4 (Long run, farmers' profits and production efficiency)** *Under the specification for the long run, a water market improves each farmer's profit thus production efficiency.*

Each farmer has always the possibility within a water market to keep his/her initial productivity, apply the same quantity of water as the status quo and sell the remaining quantity, which gives him/her a profit at least equal to his/her profit in the status quo. The improvement of each farmer's profit naturally implies the improvement of the sector's profit.

[5]Note that Inequality 4 involves now only exogenous parameters.

It remains now to check whether a water market encourages investments. We consider the investment decisions respectively in the status quo then with a water market. Then the investment decisions in both situations are compared.

**Proposition 2 (Investment decisions in the status quo)** *Under the specification for the long run, in the status quo,*

- *If $p\omega > a$ all inefficient farmers choose $\mu = 1$.*
- *If $p\omega \leq a$ all inefficient farmers choose $\mu = 1/3$, i.e., no investment is made.*

Suppose now that a water market is set up. Proposition 3 provides the investment decisions of farmers in such conditions. Before doing so, we need the following lemma.

**Lemma 1** *Under the specification for the long run, an inefficient farmer necessarily chooses productivity $\mu = 1/3$ or productivity $\mu = 1$. Thus after the investment choice, productive farmers have necessarily a productivity equal to 1.*

Lemma 1 states that an inefficient farmer actually makes his/her choice between keeping his/her initial productivity and moving to the best one. He/she never makes intermediary decisions. This is because the investment is linear w.r.t. the difference between productivities. This result allows to simplify the comparison between the water market and the status quo in terms of private investment, as it amounts to the comparison of the number of investing farmers in both situations.

**Proposition 3 (Investment decisions with a water market)** *Under the specification for the long run, let $(u_t)_{m \leq t \leq m+q-1}$ be the sequence defined by:*

$$u_t = (3/2)mp\omega\left(\frac{1}{2t(t+1)} + \frac{(m+q)}{4(t+1)^2}\right) \tag{5}$$

*Three cases are possible:*

- *$u_m \leq a$, there is a unique Nash equilibrium in which all inefficient farmers keep their productivity at its initial level.*
- *$a < u_{m+q-1}$, there is a unique Nash equilibrium in which all inefficient farmers move to productivity 1.*
- *Otherwise, there exists some integer $h$ such that $u_{m+h} \leq a < u_{m+h-1}$, in which case the set of Nash equilibria involves all the $q$-uples in which there are exactly $h$ investing farmers who move to productivity 1 and $(q-h)$ farmers that keep their initial productivity.*

From Result 5 the consideration of the effects of water markets in terms of private investments turns out to be more complicated than expected by a rough intuitive approach. In some cases water markets may dissuade farmers from investing while the same farmers would invest if no water market is set up. These findings which could not be easily guessed in advance, may be explained as follows.

With a water market, the profit of an (initially) inefficient farmer comes from production and water resale. The decision of investing in new technologies will be taken only if water resale is not very profitable. Water markets result in two contradictory effects. First a water market better reveals the value of water through the water equilibrium price, thus urges farmers to save water through adequate investments. At the same time, the possibility of water resale may dissuade farmers from production and investment. Without a water market, inefficient farmers make profit only from production. The decision of investment is taken if it is profitable in terms of production only.

In the first case ($\frac{q}{m} < \frac{5}{3} + \frac{10}{3m} + \frac{2}{3m^2}$), the proportion of initially inefficient farmers is relatively low, then the second effect is always the winner. Indeed in this case water being scarce because provided by few farmers, water resale is profitable and inefficient farmers are more willing to rely on water resale than on production, to make profit. The existence of a water market always reduces the number of investing farmers when compared to the status quo.

In the second case ($\frac{q}{m} > \frac{5}{3} + \frac{10}{3m} + \frac{2}{3m^2}$), the number of inefficient farmers is relatively high, the choice between water resale and investment-production becomes more complicated. The two effects have comparable consequences. Hence *a priori* the number of investing farmers with a water market may be greater or smaller than that number in the status quo. For sufficiently intensive investments and/or sufficiently low output or quota ($p\omega < a < u_m$), it appears that the first effect is stronger than the second one. This can be explained in a double way. Considering the production and investment side, a high intensity of investment and/or a low output price have two contradictory effects. Investment and production are not profitable as production is costly w.r.t. entries, reducing the incentive for investment. This direct effect raises water offer, lowers the water price thus making the water resale less profitable and production more attractive! An equilibrium between the two effects occurs when some farmers among the inefficient ones invest and the remaining ones continue to sell their water rights. The explanation is simpler when we view the result in terms of quotas. When the quota is low, the available water is scarce, which makes its resale interesting and lowers the incentives for investment and production within a water market.

## V. CONCLUDING REMARKS

To conclude, the claims made about the effects of water markets in the short and long run, are not always theoretically founded. Several concluding remarks and perspectives for future research may be driven from the analysis.

Water markets improving each farmer's profit thus the whole sector's profit, ensure traditional farmers' support and are likely to improve the agricultural sector's situation in countries where farmers are among the poorest people, without increasing the water

offer thus without harming the environment. The same amount of water is used more efficiently through water markets. However only traditional farmers are considered in the model. The results may change if "potential farmers" are considered. A water market may even dissuade new farmers from entering in the sector as it results in a rise of water prices, while they would be younger, more highly educated, thus more aware of the modern techniques than traditional farmers. A further interesting step to this research would be to deal with the effects of water markets considering a group of farmers of two types: traditional farmers with historical use rights and potential ones with no use rights.

However the improvement of production efficiency does not necessarily imply an improvement of total production. We indeed prove that a water market may not improve total production, which may be problematic in a scarcity or poverty context or when the considered farm good has a strategic or food security role (for instance some kinds of cereals in Tunisia).

Taking into account the transaction cost of water markets and the social cost due to the inactivity of the least efficient farmers, we prove that a water market does not necessarily improve social surplus. The welfare analysis would be more complete if the price of the farm good is endogenized and the demand side of the farm good properly taken into account. This would be another possible further research step.

Finally, a water market sometimes discourages private investments. This last result, contrary to the roughly intuitive expectations but consistent with some observations on water market experiences, proves that the short term drawbacks of a water market are not always mitigated by its long term effects.

## REFERENCES


1. Bauer C J (1997) Bringing water markets down to earth: the political economy of water rights in Chile, 1976-95. World development 25(5): 639-656.
2. Burness H S and Quirk J P (1979) Appropriative Water Rights and the E_cient Allocation of Resources. The American Economic Review 69: 25-37.
3. Burness H S and Quirk J P (1980) Economic Aspects of Appropriative Water Rights. Journal of Environmental Economics and Management 7: 372-388.
4. Bohm P and Russel C (1985) Comparative analysis of alternative policy instruments. In: Kneese and Sweeney (Eds) Handbook of Natural Resources and Energy Economics. Elsevier Science Publishers B. V.
5. Gleik P H (1998) The world's water: the biennal report on fresh water resources 98/99. Island Press. 17
6. Hearne R R and Easter K W (1995) Water allocation and water markets: an analysis of gains from trade in Chile. World Bank technical paper. No 315.
7. Howe C W, Schurmeier D R and Douglas ShawWJR (1986) Innovative approachs to water allocation: the potential for water markets. Water resources research 22(4): 439-445.
8. Jung C H, Krutilla K and Boyd R (1996) Incentives for Advanced Pollution Abatement Technology at the Industry Level: An Evaluation of Policy Alternatives. Journal of Environmental Economics and Management 30(1): 95-111.
9. Lahmandi-Ayed R and Matoussi M S (2003) Selection through water markets. In: Koundouri P, Pashardes P, Swanson T and Xepapadeas A (Eds). Economics of Water Management in

Developing Countries: Problems, Principles and Policies. Edward-Elgar Publishers. (ISBN: 184376122X).
10. Malueg D A (1989) Emission Trading and the Incentive to Adopt New Pollution Abatement Technology. Journal of Environmental Economics and Management 16(1): 52-57.
11. Milliman S R and Prince R (1989). Firm Incentives to Promote Technological Change in Pollution Control. Journal of Environmental Economics and Management 17(3): 247-265.
12. Ministry of agriculture of Tunisia (1998). A water sector study, by Bechtel-Scet Tunisie.
13. Ministry of agriculture of Tunisia (2000). Eau 21: Stratégie à long terme du secteur de l'eau en Tunisie (2030).
14. Provencher B (1993). A Private Property Rights Regime to replenish a groundwater aquifer. Land Economics 69: 325-40.
15. Provencher B and Burt O (1994). A Private Property Rights Regime for the Commons: the case for Groundwater. American Journal of Agricultural Economics 76: 875-888.
16. Requate T (1998). Incentives to innovate under emission taxes and tradeable permits. European Journal of Political Economy 14: 139-165.

## APPENDIX: PROOFS

**Proof of Result 1.** First note that $x_i^s = d_i(0)$. Inequality (1) is then equivalent to $\sum_{i=1}^n d_i(0) > \Omega$. Equation $pf_i'(x_i) - C_i'(x_i) = p_e$ defines implicitly $\tilde{x}_i(p_e)$ as a continuous decreasing function of $p_e$. $d_i$ is then a continuous non-increasing function of $p_e$, and so is $\sum_{i=1}^n d_i$. On the other hand there exists $\bar{p}_e$ such that for all $p_e > \bar{p}_e$, for all $i = 1, .., n$, $pf_i'(0) - C_i'(0) - p_e < 0$, then $\pi'(x_i) < 0$ for all $x_i \geq 0$, which implies $d_i(p_e) = 0$, so $\sum_{i=1}^n d_i(p_e) = 0$. Consequently, there exists a unique $p_e^* > 0$ such that $\sum_{i=1}^n d_i(p_e^*) = \Omega$. ∎

**Proof of Result 2.** As $d_i(p_e)$ maximizes the profit of farmer $i$ with a water market, it ensures to him/her a better profit than $d_i^s$ his/her demand in the status quo, which is written as

$$pf_i(d_i(p_e)) - C_i(d_i(p_e)) + p_e(\omega_i - d_i(p_e)) \geq pf_i(d_i^s) - C_i(d_i^s) + p_e(\omega_i - d_i^s).$$

As $p_e(\omega_i - d_i^s) \geq 0$ since $d_i^s \leq \omega_i$, we have

$$pf_i(d_i^s) - C_i(d_i^s) + p_e(\omega_i - d_i^s) \geq pf_i(d_i^s) - C_i(d_i^s),$$

implying

$$pf_i(d_i(p_e)) - C_i(d_i(p_e)) + p_e(\omega_i - d_i(p_e)) \geq pf_i(d_i^s) - C_i(d_i^s),$$

which says that the profit of farmer $i$ is better under water market than in the status quo.

Summing these inequalities, together with $\sum_{i=1}^n d_i(p_e) = \sum_{i=1}^n \omega_i$, we prove that a water market improves the profit of the whole sector. ∎

**Proof of Result 3.** With these values, we have first: $x_i^s > \omega_i$, so that in the status quo $d_i^s = \omega_i = \Omega/2$ and total production equals $\mathcal{P}^s = (\delta_1 + \delta_2)\Omega/2$.

With a water market, we have $\delta_2 - \delta_1 < \frac{2c_2\Omega}{p}$, which ensures the activity of both farmers at equilibrium. Demands of farmers are respectively given by the following:







London Journal of Research in Science: Natural and Formal

$$d_1 = \frac{p\delta_1 - p\delta_2 + 2c_2\Omega}{2(c_1 + c_2)}$$

and

$$d_2 = \frac{p\delta_2 - p\delta_1 + 2c_1\Omega}{2(c_1 + c_2)}.$$

Total production is then given by

$$\mathcal{P}^w = \delta_1 d_1 + \delta_2 d_2 = \frac{p(\delta_2 - \delta_1)^2 + 2\Omega(c_2\delta_1 + c_1\delta_2)}{2(c_1 + c_2)}.$$

$\mathcal{P}^w < \mathcal{P}^s$ is equivalent to $\delta_2 - \delta_1 < \frac{\Omega(c_2 - c_1)}{p}$, which holds with the chosen values of the parameters. ∎

**Proof of Result 4.** Denote by $d_i(\mu_i, \mu_{-i})$ the farmer $i$'s demand of water when he/she chooses $\mu_i$ and the other farmers choose $\mu_{-i}$. Denote by $\mu^*$ the $q$-uple of productivities chosen by farmers at equilibrium. We have the following:

$$\begin{aligned} pf_i(d_i(\mu_i^*, \mu_{-i}^*)) - C_i(d_i(\mu_i^*, \mu_{-i}^*)) - I(\mu_i^*) + p_e(\omega_i - d_i(\mu_i^*, \mu_{-i}^*)) & \\ \geq pf_i(d_i(\delta_1, \mu_{-i}^*)) - C_i(d_i(\delta_1, \mu_{-i}^*)) + p_e(\omega_i - d_i(\delta_1, \mu_{-i}^*)) & \quad (6) \\ \geq pf_i(d_i^s) - C_i(d_i^s) + p_e(\omega - d_i^s) & \quad (7) \\ \geq pf_i(d_i^s) - C_i(d_i^s). & \quad (8) \end{aligned}$$

Inequality 6 holds as $\mu_i^*$ is a best reply to $\mu_{-i}^*$ thus is better than the initial productivity $\delta_1$. Inequality 7 holds as quantity $d_i(\delta_1, \mu_{-i}^*)$ is chosen to maximise farmer $i$'s profit within a water market thus is better than $d_i^s$ the farmer's demand in the status quo.

This proves that a water market improves each farmer's profit.
Now summing the inequalities

$$pf_i(d_i(\mu_i^*, \mu_{-i}^*)) - C_i(d_i(\mu_i^*, \mu_{-i}^*)) - I(\mu_i^*) + p_e(\omega_i - d_i(\mu_i^*, \mu_{-i}^*)) \geq pf_i(d_i^s) - C_i(d_i^s),$$

we obtain

$$\sum_{i=1}^{n} pf_i(d_i(\mu_i^*, \mu_{-i}^*)) - C_i(d_i(\mu_i^*, \mu_{-i}^*)) - I(\mu_i^*) \geq \sum_{i=1}^{n} pf_i(d_i^s) - \sum_{i=1}^{n} C_i(d_i^s).$$

**Proof of Proposition 2:** Denote by $\mu$ the productivity chosen by an inefficient farmer. His/her profit when he allocates quantity $x$ to production, is given by:

$$\pi = p\mu x - cx^2 - a(\mu - 1/3)$$

His profit is maximum at $\bar{x} = \omega$. Indeed, first order condition yields: $x^* = p\mu/2c \geq p/6c$, to be compared to $\omega$. But relation (2) equivalent to $\omega = pm/4c(m + q)$ together with inequation (3), implies $x^* \geq \omega$.

After calculations, the profit is given by:

$$p_e = (\frac{1}{t+1})[p(\mu+\alpha) - 2c(t+1)\omega],$$

$\alpha$ being the sum of productivities of all the other productive farmers.
The productive quantity is given by:

$$x = \frac{pt}{2(t+1)c}\mu - \frac{p}{2(t+1)c}\alpha + \omega$$

The total profit of the considered farmer is given by:

$$\pi(\mu) = [p_e(\omega - x) + p\mu x - cx^2] - a(\mu - 1/3)$$

The coefficient of $\mu^2$ has the same sign as $1 - \frac{t+2}{2t+2}$ which is non negative for all $t \geq 0$.

Hence, the profit of the farmer is a continuous function that is linear decreasing then convex. It reaches its maximum at 1/3 or at 1. ∎

**Proof of Proposition 3:** Consider an inefficient farmer $i \in \{1, .., q\}$. Let $t$ be the number of productive farmers (in the first and the second group other than the considered one). According to Lemma (1), they have necessarily a productivity equal to 1. Farmer $i$ makes his/her choice between $\mu_i = 1/3$ and $\mu_i = 1$.

If $\mu_i = 1/3$, then the equilibrium water price is equal to

$$p_e = \frac{p}{t}t - \frac{2c\Omega}{t} = p - \frac{2c\Omega}{t}.$$

The corresponding profit is given by:

$$\pi(1/3) = (p - \frac{2c\Omega}{t})\omega$$

using the relation $\frac{c\Omega}{mp} = 1/4$, this profit becomes

$$\pi(1/3) = (1 - \frac{m}{2t})p\omega.$$

If $\mu_i = 1$, the equilibrium water price is equal to

$$p_e = p - \frac{2c\Omega}{t+1},$$

and the productive quantity is equal to

$$x_i = \frac{\Omega}{t+1}.$$

The corresponding profit is equal to

$$\pi(1) = (p_e(\omega - x) + px - cx^2) - (2/3)a$$







London Journal of Research in Science: Natural and Formal

Using Equality (2), this profit is equal to

$$\pi(1) = p\omega(1 - \frac{m}{2(t+1)}) + p\Omega(\frac{m}{4(t+1)^2}) - (2/3)a.$$

The difference is then given by:

$$\pi(1) - \pi(1/3) = mp\frac{\omega}{2t(t+1)} + mp\frac{(m+q)\omega}{4(t+1)^2} - (2/3)a.$$

Farmer $i$ moves to productivity $\mu_i = 1$ if $a < u_t$.

Note that $(u_t)_{m \leq t \leq m+q-1}$ is a decreasing sequence. Three cases are then possible:

If $u_m \leq a$, then for all $t$, $u_t \leq a$. This implies that whatever the number of other investing farmers, Farmer $i$ has no interest to invest.

If $a < u_{m+q-1}$ then for all $t$, $a < u_t$. This implies that whatever the number of other investing farmers, Farmer $i$ invests.

Otherwise, there exists some integer $h$ such that $u_h \leq a < u_{h-1}$. In this case the best reply of Farmer $i$ is to move to productivity 1 if the number of other productive farmers is less or equal to $h-1$, and to keep his/her productivity if this number is greater or equal to $h$. ∎

**Proof of Result 5.**

1) When $\frac{q}{m} < \frac{5}{3} + \frac{10}{3m} + \frac{2}{3m^2}$, we have: $u_{m+q-1} < u_m < p\omega$.

- When $a < p\omega$ all farmers invest in the status quo. However with a water market all of them invest only when $a < u_{m+q-1}$. The number of investing farmers with a water market is at most equal to $q-1$ when $u_{m+q-1} < a$.
- When $a > p\omega > u_m > u_{m+q-1}$, whether or not a water market is implemented, no farmer invests.

2) When $\frac{q}{m} > \frac{5}{3} + \frac{10}{3m} + \frac{2}{3m^2}$, we have: $u_{m+q-1} < p\omega < u_m$.

Denote by $n_{wm}$ the number of investing farmers with a water market and by $n_s$ the number of investing farmers in the status quo. Results are summarized in the table below:

| $a$ | $n_{wm}$ | Comparison | $n_s$ |
|---|---|---|---|
| $a < p\omega$ | $\leq q$ | $\leq$ | $q$ |
| $p\omega < a < u_m$ | $> 0$ | $>$ | $0$ |
| $a > u_m$ | $0$ | $=$ | $0$ |

# Physically Defining Life: A Thermodynamic Systems Analysis of Biology

*Dr. Stephen Palmer*

## ABSTRACT

This paper applies recent advances in analysing systems behaviour based on thermodynamics to investigating the physical basis of biology and so provide a physical definition of life. The definition of life provided also provides a physical basis for Dawkins's selfish gene theory. The systems analysis of prokaryote evolution and development herein also describes an example of Dawkins's extended phenotype emerging during prokaryote evolution. This paper also identifies the biophysical basis for the emergence of ecological 'r' and 'K' reproductive strategies in prokaryotes. Finally, part of this analytical approach is applied to recent work on the origin of life and used to describe its alignment with a particular hypothesis for the origin of life on Earth.

*Keywords:* thermodynamics, systems analysis, definition of life, extended phenotype.

*Classification:* LCC Codes: QH331, QH324.2, QH501

*Language:* English`

Great Britain Journals Press

LJP Copyright ID: 925614
Print ISSN: 2631-8490
Online ISSN: 2631-8504

London Journal of Research in Science: Natural and Formal

Volume 23 | Issue 10 | Compilation 1.0

# Physically Defining Life: A Thermodynamic Systems Analysis of Biology

Dr. Stephen Palmer

## ABSTRACT

*This paper applies recent advances in analysing systems behaviour based on thermodynamics to investigating the physical basis of biology and so provide a physical definition of life. The definition of life provided also provides a physical basis for Dawkins's selfish gene theory. The systems analysis of prokaryote evolution and development herein also describes an example of Dawkins's extended phenotype emerging during prokaryote evolution. This paper also identifies the biophysical basis for the emergence of ecological 'r' and 'K' reproductive strategies in prokaryotes. Finally, part of this analytical approach is applied to recent work on the origin of life and used to describe its alignment with a particular hypothesis for the origin of life on Earth.*

*Keywords:* thermodynamics, systems analysis, definition of life, extended phenotype.

*Author:* Stantec Ltd., Stantec House, Kilburn Court, Birchwood, Warrington, U.K.

## I. INTRODUCTION

Recent advances in theoretical quantum thermodynamics have enabled new insights into how quantum changes can emerge into physical reality via decoherence (Palmer, 2019). They have also clarified what entropy is.

At the quantum level, a change of microstate requires energy redistribution between an object quantum system and those quantum systems constituting its environment.

The physical elements of quantum microstates follow information systems behavior as described by the statistical mechanics of Shannon information theory:

$$H = - \Sigma p_i \log p_i \quad (1)$$

(where H = Shannon measure of information (the missing information equaling uncertainty) and $p_i$ is the probability of any given microstate)

When the energy distribution within the microstates of a simple closed, isolated physical system is described, the Shannon information description of the system then re-emerges in the form:

$$S = k_B \ln \Omega \quad (2)$$

(where S = system entropy (units of energy /temperature E/T), $k_B$ = Boltzmann constant (energy/temperature), $\Omega$ = number of microstates possible for macroscopic constraints (i.e. system total energy E).

This is Boltzmann's definition of entropy, significantly predating Shannon's information theory. The relationship between these two descriptions is a consequence of physical quantum microstate information theory's statistical mechanics for energy distribution within the system. Temperature is a metric of the energy distribution within the system in which the entropy is the uncertainty of how energy is distributed within that isolated system.

## II. CLARIFYING AND UNDERSTANDING ENTROPY

The significance of these recent advances is that they allow clarification of what entropy is and importantly, what it is not.

Entropy at the microstate level is simply missing information (uncertainty) in respect of the distribution of the agent of physical microstate change, energy.

There is no element of order or disorder implied by entropy. The association of entropy with order and disorder is a common mistake still regularly seen in scientific publications, but it is entirely erroneous (Ben Naim, 2008; Palmer 2022) leading to misinterpretations of the consequences of entropic system behavior.

The quantum level entropy as microstate uncertainty emerges at the classical level as uncertainty about energy distribution in the form of *energy dissipation*, during 'change' in a classical system.

For systems to change they need to consume free energy (usually termed 'exergy') to carry out work. The physical information of a system s is described by:

$$H = B/T_o \tag{3}$$

(where H = Shannon measure of information (=uncertainty = missing information), B = free energy (exergy) of the system and $T_o$ is the temperature of the systems environment)

Consequently, the physical state and physical information regarding the state of a system is related to how free energy (exergy) is distributed in the system compared to the energy distribution (temperature) of the systems' environment.

This is a key concept in thermodynamic systems behavioural analysis - the physical information defining a system is that which distinguishes that system from its environment. Physical system information is relative; it is the information that distinguishes the system from its background (*its physical environment*).

When we analyse the behaviour of biological systems we are dealing with *open, interacting systems which are also chemical systems*:

$$H = E + P_o V - \Sigma\rho_{io} N_i / T_o \tag{4}$$

(where the system uncertainty $H$ is related to the distribution of molecules in an environment with a number of moles $N_i$, chemical potential $\Sigma\rho_{io}$, distributed in volume $V$ at pressure $P_o$ and temperature $T_o$, with energy E)

The thermodynamic information for a system change $I$ is defined by the loss of information that occurred when the system changed to state $S_o$ in which it is indistinguishable from its environment (Tribus and McIrvine, 1971)

$$I = S_o - S \tag{5}$$

The interactions producing microstate changes in an object-system are stochastic (probabilistic). The physical information of a particular change of state in a physical system is a record of its last interactions between the object-system and the systems that populate its environment.

The conditional probability distribution for future states of the interacting systems depends on the present state of the systems. Physical and chemical systems follow *Markovian* behavior wherein information about past interactions between a system and its environment is *dissipated*.

## III. DEFINING LIFE IN PHYSICAL SYSTEM TERMS

Life and living systems are typically defined in terms of their observed common behaviors across living systems such as growth, reaction to stimuli, metabolism, energy transformation and reproduction.

Living systems are capable of adaptation and evolution through successive generations, which arises from 'imperfect' system replication. Biological systems are distinguishable from physical and chemical systems by their attribute of memory. For life on Earth, the period for which the agent of memory is the gene in the form of nucleic acids (DNA and RNA), extends at least as far back as the Last Universal Common Ancestor of prokaryotes (LUCA) and probably beyond.

System memory for a physical system arises from a biological system being able to replicate itself within its environment subject to the pressures the environment exerts on the systems success in replication, so a 'system' with memory could first emerge as a self-replicating physical structure or as a self-replicating chemistry.

On a physical system behavioural basis, a universal system definition for biological systems and life is:

*'A system (chemically based in known biological systems) with memory which is utilized for environmental fitness, with fitness defined by success in replicating the system in its environment'.'*

This thermodynamically referenced definition of life emphasizes that the difference between biological systems and natural physical and chemical systems is biological systems' attribute of memory. The key distinction between life and physical or chemical systems is that biological systems are *non-Markovian* in their system behaviour, due to their replication creating a memory which is transferable between generations, which allows them to adapt to their environment. The attribute of memory makes biological systems *learning systems* in physical information terms. This paper focuses on the biophysical aspects of prokaryotes as an example of the foundational physical systems aspects of biology because prokaryotes are the first emergent biotype for life on Earth and because there is far less distance in prokaryotes between genotype and phenotype and form and function.

The information content of a system obviously describes its physical state and any *change* of state in a physical system is accompanied by a change in the system information. A closed system that does not change is at thermodynamic equilibrium and is *indistinguishable* from itself at a previous point in time.

For open interacting systems such as biological systems, a system at equilibrium is indistinguishable from its background. For such systems where the physical information of the system is different to its background when the system is not at equilibrium with its background.

The profound significance of the relationship $H = B/T_o$ (equation 3) is that a physical system's information is the *difference* in information between the physical system being observed and its environment- the information that *distinguishes* it from its environment.

Physical and chemical systems compete for exergy (free energy) in a given environment to be able to change state but the interaction being observed is Markovian. There is no information carried over to the next interaction for the interacting physical or chemical system. *Markovian behaviour dissipates information.*

In contrast, the defining memory attribute of biological systems allows information on the systems interactions with its background (environment) to be passed down generations of the self-replicating system. There is a second critical system behavioural characteristic being exhibited here: system

self-replication creates the basis for memory, but memory itself is essential for a system to be able to *utilise* information.

The successive (generational) development of information in an observed biological system also has profound implications for how physical structural change can accrue over time. The mathematical behavior of simple systems under persistent, successive positive feedback (in this case feedback on success of replication arising from fitness for replication in the environment) is one that leads to emergence of complex systems (Holland, 1992, Holland 1996, Holland 1998).

This particular characteristic is a key consideration in analysis of emergence of life on Earth (or elsewhere, as these are universal physical principles). System self-replication is the basis for memory, so the earliest emergence of life must be associated with some form of self-replication of physical -chemical systems.

Another key attribute required for a successful self-replicating chemistry to exhibit utilization of information of the information its stores is for the self-replicating system to be incrementally modifiable (e.g. the system needs to have a means for variation to arise its memory). In systems terms, this could be provided by generic mechanisms such as errors in the systems' self-replication or from exchange of information between systems.

These are the physical systems behavioral constraints which the classical biological elements of genotype and phenotype have to act within. A physical structural type of biological system has its genotype as its memory and the agent for system learning fitness to replicate in different environments is the gene (Dawkins, 1976).

The definition of life provided in this paper implies that there is only one physical systems agency for feedback on object- system replicative success. It is the observed systems environment (which is itself a population of other physical, chemical plus biological systems, after the emergence of life).

Physical systems' analysis provides the physical basis for the biologically universal utility of Dawkins' selfish gene' concept. Biological systems are not possible without memory and the success of a gene is simply defined by its ability to self-replicate. On a physical basis, each gene represents an agent of memory competing for the resources needed to optimize its generational self-replication. A physical system approach also allows us to clarify *phenotype* in physical terms. The phenotype is simply the physical structural vehicle for the system memory (gene's) intergenerational replication.

The physical structure of that vehicle (organism structure) encodes its history of actionable information relative to the environment, up to the point of historic structures still retaining present-day utility. If a biological system has memory capacity constraints, it is the environment (*via* its resources for replication and competition for them) that will dictate how that memory is most efficiency utilized to secure replicative fitness (i.e. determine whether genes are retained or lost from the overall available capacity).

This definition of biological systems implies that adaptation to the environment defined by attaining replicative success is the principal system feedback confirming biology. It also implies that a biological system does not to inherently need to metabolize itself: if a biological system can utilize (parasitize) a biological host-system to carry out the work of replication then it needs to sustain and seek far less resources from the environment (but is then of course dependent on host availability in its environment). This paper will explore how critical management of resources to replicative success within biology and how deeply those strategies and tactics for it are conserved, given that they emerge and are generic in prokaryotes.

From the definition of life provided by this paper, viruses are definitively biological systems. My previous reference to parasitism, even applied to a viral biological system strategy, does not imply that only the virus gains. Deeply interactive biological system relationships often have some degree of return to both participants and it should be noted that a virus-host cell interaction also introduces a basis for genetic recombination (horizontal gene transfer), which represents information transfer and acquisition for the host organism.

From consideration of the implications of physical information and how redistribution of energy is the agency for physical state change, we can now also consider Dawkins's 'selfish gene' concept (Dawkins, 1976)and how it aligns with a physical definition of life.

At whatever point early in the emergence of life where a specific form of chemical memory emerges, it will dominate information retention in a biological system and intergenerational information utilization. *From a system viewpoint, the gene is the agent of intergenerational memory of interactions with the environment and the organism is a vehicle for it.*

However, a gene being selfish in terms of its purpose of self-replication should not be confused with the system behaviour needing to be selfish. The purpose of adapting system behavior in relation to the environment is replicative success and the growth strategies and resource acquisition tactics needed to meet that goal will be selfish under some environmental conditions but cooperative under others.

A genome will evolve symbiotic behaviour under generations spent in certain environmental conditions including resource limitation and variability in resources and competition for resources, as will be demonstrated below in a case study of prokaryote evolution.

The critical difference between biological systems and physical or chemical systems is biological systems' capability for utilization of information. Biological systems are learning systems, whose reference point for distinguishing survival-information from survival-misinformation (noise) is its *environment* (Palmer, 2019).

*The biological cell and the non-equilibrium thermodynamics of its growth.*

Energy redistribution including consumption of free energy is required for systems to change state. The relationship between form and function for successful information (gene) replication of biological systems is a continuous, dynamic process. It is further complicated by the fact that biological systems in turn affect their environment while maximising their potential to replicate within it. The process requires a continuous energy flux through a biological system to maintain an individual system (organism) until it has successfully replicated, in order to propagate the genome through successive physical *vehicle* (phenotype) generations (Dawkins, 1982). On a simple systems basis, once the genome is successfully propagated the individual phenotype (organism) itself is redundant and the individual phenotype can fall back into equilibrium with its environment (its death) without jeopardizing the success of the genotype in replicative terms.

In system terms, the utility of the information system also needs to provide variation in information content in order to provide a basis for creating new genotypic variants relative to its environment. The sources of variation in the information system we are familiar with in the emergent phenotypic prototypes for life on Earth (i.e. LUCA and the prokaryotes) are; mutation, gene loss, error and even recombination via Horizontal Gene Transfer (HGT).

A biological system's most universal structural unit form is the cell. When LUCA emerges in terrestrial evolution, genetic code is provided by DNA and RNA. LUCA's cell structure consisted of a membrane and wall, with the structures for energy generation being part of the membrane (Martin & Russell,

2003; Lane, 2015). Energy generation for biosynthetic activity supporting anabolism (including growth and genome reproduction) is provided by catabolism.

Catabolism is coupled to anabolism to drive anabolism and growth (Fig. 1).

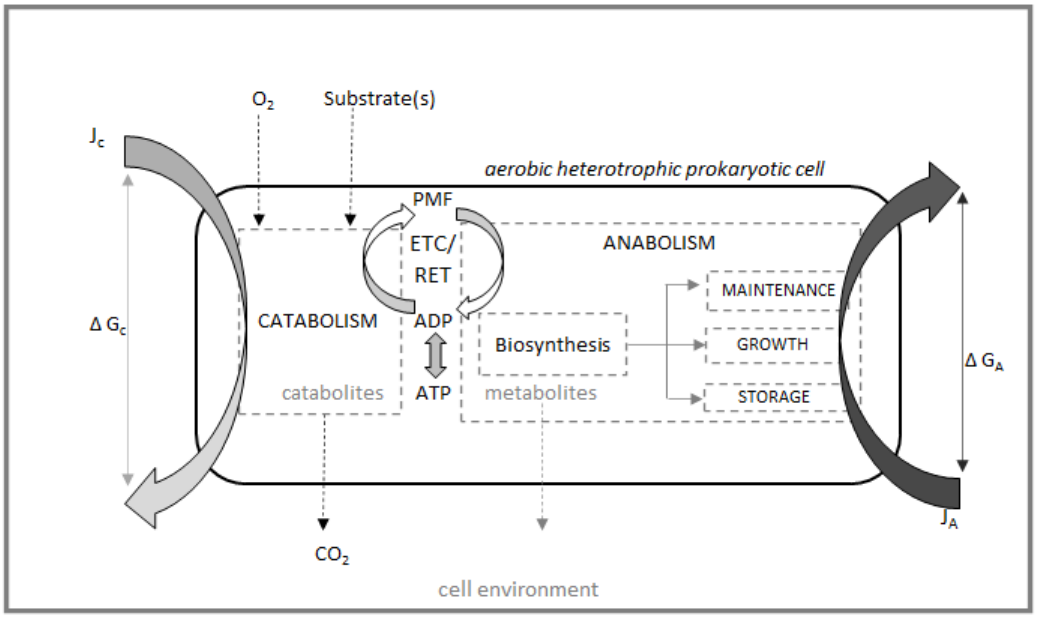


*Figure 1:* Systems analysis diagram for a prokaryotic cell

A prokaryotic cell system diagram for an aerobic heterotrophic prokaryote. The cell can sustain itself far from thermodynamic equilibrium by coupling the energy generated from catabolism to anabolic work (growth, cell maintenance, substrate storage). This coupling of catabolism to anabolism sustains a driving force $J_A$ for anabolic activity from the energy sink of force $J_c$. Force $J_c$ is maintained by the exergy provided by Gibbs energy released by catabolism (ΔGc) which in turn creates a driving force $J_A$ for cell reproduction (growth). The origin of force $J_c$ counterbalancing force $J_A$ is the system entropy balance and the system attempting to return to equilibrium with its environment. Two fundamental reproductive (growth) strategies then arise from thermodynamic constraints: growth at maximum reproductive rate, in which anabolic energy and resources are diverted mainly to fast reproduction of a basic viable cell, or growth based on reproducing more resilient cells with greater longevity potential based on a higher proportion of anabolic energy into maintenance, regulation and storage in which cell mass (yield) is higher. These two reproductive strategies can be identified with the ecological theory of 'r' and 'K' strategies for reproduction (Reznick *et al,* 2002) with 'r' strategy for maximum rate of cell reproduction being competitive when resources are not limited and the 'K' strategy of production of higher mass, more resilient, cells.

The entropy balance for reacting chemicals *j* in a mixed flow through environment at constant temperature and pressure is:

$$S_{prod} = \Sigma j\ -\Delta r_j G/T\ \xi j + W/T + \Sigma j\ (\mu i_{in}/T - {}_i\ \mu i_{out}/T)\ \ nj,_{in} \qquad (6)$$

(where S is the entropy produced from the Gibbs reaction energy $-\Delta rjG$ , W work done, 'T' is temperature, $\mu i$ the chemical potential of the 'i'th component, ξj = rate of the jth chemical reaction and $n_{j\ in}$=- the influx flow) (von Stockar, 2013)

For two flux forces exerted across a (prokaryotic) cell both are proportional to their conjugate force 'Zi'**:**

$$J_i = L_i . Z_i \quad (7)$$

(where L*i* is a constant for the flux) (Von Stockar, 2013)

For the flux forces exerted across a (prokaryotic) cell between a bioenergetic catabolic reaction coupled to an anabolic process, assuming the flux for catabolism is designated $J_c$ and that for anabolism designated $J_A$, the anabolic process can be driven against its driving force by it being *coupled* to the catabolic reaction as shown in Fig.1 below.

Growth-coupling is not fully complete *i.e.* 100% between catabolism and growth-anabolism because the cell also uses other biosynthetic processes in addition to cell replication (growth) to manage entropy (cell maintenance processes) and manage resources (manage starvation risk) which is described in the Herbert -Pirt equation:

$$1/Y = 1/Y_{max} + m/\mu \text{ (Von Stockar, 2013)} \quad (8)$$

(where Y = biomass yield from catabolism, $Y_{max}$ = maximum biomass yield from catabolism, $\mu$ is the growth rate and m is the energy used in cell maintenance processes)

Open system thermodynamics for a cell as illustrated in Fig 1 allow derivation of a cell replication (growth) rate in relation to the rate of catabolic substrate consumption:

$$r = L\, RT \ln c + C \text{ (Von Stockar, 2013)} \quad (9)$$

(where r = cell growth rate, L = coupling coefficient for catabolism and anabolism, C = catabolic substrate concentration, c = catabolic substrate saturation concentration, R = universal gas constant, T = temperature)

Equation (9) provides a relationship between growth and catabolic substrate removal kinetics which closely fits that of Monod growth kinetics;

$$\text{Monod kinetic relationship } \mu = \mu_{max}(S/(K_s + S)) \quad (10)$$

for which Substrate removal = $- r_s = \mu(X/Y_s) . (S/(K_s + S))$

(where -r = catabolic substrate removal rate , $\mu$ = specific growth, $\mu_{max}$ = maximum growth rate, X = cell biomass, Y = biomass yield, S = catabolic substrate concentration, $K_s$ = substrate half-saturation coefficient)

The Monod relationship arose from Monod's observation (Monod, 1950) that in the exponential growth phase, prokaryote biomass formation increased in proportion to substrate consumption. The growth yield '$Y_s$' is defined by the catabolic substrate electron consumption per amount of biomass produced. This varies for different substrates with their associated Gibbs free energy and the efficiency of energy transfer directly into cell growth, balanced by any demands for cell maintenance (Equation 8). Monod's work illustrated the function of the prokaryotic gene in providing the feedback between the environment and prokaryote with gene regulation then giving the prokaryote options from the genome in its response to changing environmental conditions.

*Evolutionary feedback on cell bioenergetic constraints*

Prokaryote bioenergetic outcomes are a balance between irreversible thermodynamic constraints, resource availability and variation in the environment, all of which in turn shapes the genome through natural selection. A high degree of physical structural complexity emerges from a self-replicating information system learning to adapt to its environment even at the level of the prokaryotic cell. Even

this requires its living systems to maintain themselves continuously at a significant distance from equilibrium from their environment while alive.

When there is little or no resource limitation, including competition for substrates and resources, if the cell and its genome can sense this is the state of its environment it can express a phenotype focused on the fastest possible reproduction of the prokaryotic cell. Alternatively, if sensing determines that the ratio of resources to cells for the species is below a certain threshold value, anabolic activity and reproduction can more broadly disperse energy and resources between cell reproduction and increased cell resilience from more investment of resources into maintenance and storage (Bachmann *et al*, 2016).

Figure 2 below illustrates these reproductive alternatives. The sensing system that provides the shift between maximum growth rate (termed 'r' strategy in ecological 'r' and 'K' theory) and more resilient cells (K strategy; higher biomass yield) is *quorum sensing*.

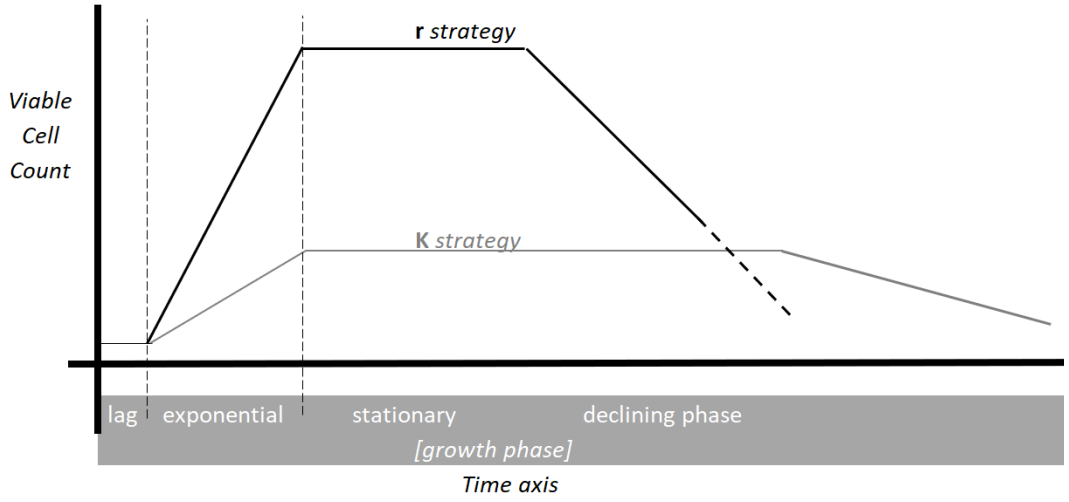


*Figure 2:* Prokaryote principal growth (reproduction) strategies.

Prokaryotes can regulate their cells to grow under two different reproductive strategies which arise from prokaryote cell biomechanical constraints. Under totally unlimited growth conditions (such as unlimited substrate chemostat experiments in which prokaryotes will grow as single cells), prokaryote growth can follow a strategy of maximum rate of minimum viable cell reproduction in order to maximize its numbers and outcompete other species for space. This **'r'** strategy supports maximum consumption of resources and maximum rate of individual cell reproduction (equivalent to Krefts 'ego' strategy (Kreft, 2004)). Prokaryotes can also use *quorum sensing*, an assessment of cell to resource density, to switch to a more *resilient phenotype* in which the cell has increased energy and resource input into maintenance, regulation and storage, which produces cells with higher biomass yield. This 'K' strategy produces more resilient cells providing the prokaryote population (species) with a higher probability of surviving for longer.

However, when resources become limited, the optimum survival strategy shifts to maximising the longevity of the population of the phenotype, making more efficient use of resources to conserve them for longer. The longevity of the population of that phenotype, optimizes yield towards that outcome via the 'K' strategy, where catabolic Gibbs free energy can be redistributed across work on maintenance and storage as well as cell growth (reproduction).

$$\Delta_r G_s = (1\text{-}Y) \,.\, \Delta_r G_{cat} + Y \,.\, \Delta_r G_{an} \text{ (Von Stockar, 2013)} \qquad (11)$$

(where $\Delta_r G_s$ = catabolic substrate Gibbs energy, Y = biomass yield from anabolic process growth coupled to catabolism, $\Delta_r G_{cat}$ = catabolic energy, $\Delta_r G_{an}$ = anabolic energy).

The Gibbs free energy driving cell activity has both an enthalpic and entropic component with the balance differing according to the form of catabolism or energy input i.e. organic carbon aerobic or anaerobic catabolism, autotrophic catabolism, fermentation or photosynthesis):

$$\Delta_r G = \Delta_r H - T\Delta_r . S \text{ (Von Stockar, 2013)} \quad (12)$$

(where $\Delta_r G$ = catabolic Gibbs free energy, $\Delta_r H$ = system enthalpy part of entropy (heat energy dissipated to environment) and $T\Delta_r . S$ represents system entropy exported to the environment as high entropy metabolites (e.g. $CO_2$ in example given in Fig 1, *etc*)

The outcomes shown in Fig.2 arise from both high bioenergetic thermodynamic driving force and high metabolic rates in maximising the rate of cell replication in the 'r' strategy. However, in a resource limited this high level of resource dissipation per individual cell can lead to competitors with a lower metabolic rate (K strategy) and associated higher resource efficiency persisting for longer as a species.

This means that almost all prokaryotes' $\Delta_r G$ runs in a zone that represents a *balance* between biomass yield efficiency and individual cell replication rate (von Stockar, 2013). Optimizing genome population survival under resource limitation can lead to other tactics in addition to selection of a Y(ield)-based growth strategy (de Mattos &Neijissel, 1997; Wang & Post, 2012, Gonzalez *et al*, 2009).

Prokaryotic cells need not fully couple catabolism to reproductive anabolism, as the reproduction K strategy illustrates. Under a K strategy a prokaryotes' anabolic activity can include more investment of energy and resources in cell maintenance, regulation and storage which results in population longevity being more probable.

Extreme examples of the latter diversion of energy into maintenance and storage that support a 'K' reproductive strategy are now known, in which there is no anabolic energy passed into reproduction. For example, some prokaryotes from deep Earth environments which have very few resources available in their environment have *minimal* metabolism such that even single cells are very long-lived (Bradley *et al*, 2018). Such extreme-environment prokaryotes are likely to represent evolution from a 'K' growth strategy which has geared cell metabolism towards minimal maintenance until the environment again becomes rich in catabolic substrates.

Further bioenergetic biomechanical limitations affecting replication rate arise from the efficiency of energy transfer through the cell's Electron Transport Chain (ETC)and Reverse Electron Transport (RET) where a prokaryote metabolism requires RET. The length of the cell ETC contributes to its inefficiency in energy transfer as described by Heijnen (2013:

$$\text{max. ETC} = 3 \exp [(-69000/R)(1/T - 1/298K)] \quad (13)$$

(where R = universal gas constant, T = temperature (K))

The maximum electron flow rate (mol e/hour) along an ETC is a function of the catabolic substrate 'C' consumption in reaction with its electron donor or acceptor. This leads to a relationship to maximum growth rate in relation to ETC efficiency:

$$\mu_{max} = 3 ((\Delta G_{cat} / y_D^- - m_G)/a_G) \exp[(-69000/R)(1/T - 1/298K)] \quad (14)$$

(where $\mu_{max}$ = prokaryote maximum growth rate, $y_D$ = electron supply from catabolic substrate which releases $\Delta G_{cat}$ Gibbs free energy from the prokaryote catabolism (per mol electron donor), $m_G$ = Gibbs energy diverted to maintenance $a_G$ = Gibbs energy required to biosynthesize 1 mol Carbon, R = universal gas constant, T = temperature (K)) (Heijnen, 2013)

The bioenergetic returns from catabolism are a function of the carbon source (as in Fig 1) or the energy source used and its electron donor for the catabolic reactions.

The cost of anabolic biosynthesis '$a_G$' is affected by the growth conditions (i.e. anaerobic versus aerobic) and the electron donor. Where the electron donor results in an anabolic Gibbs energy demand '$a_G$' which is significantly more than zero, such as in autotrophic carbon growth (autotrophic methanogenesis), there is a need for reversed electron transport (RET) along the ETC.

The 'biomechanics' of catabolism bioenergetics also include efficiency considerations related to the length of the catabolic pathway.

For extended pathways, kinetic inefficiencies can arise from leakage or other inefficiencies including operating at elevated concentrations, many enzymatic steps, and their energy losses.

Kinetic theory of catabolism (Costa *et al*, 2006) assumes that natural selection on energy returns from catabolism is driven towards maximal ATP generation, which is favored by optimum catabolic substrate conversion and minimum path length. Costa *et al* (2006) show how the limitations from catabolism in nitrification arising from kinetic theory of optimal pathway length. This explains why prokaryote nitrification has evolved into a two-stage process (with ammonia oxidising prokaryotes feeding nitrite oxidising prokaryotes), due to the shortened catabolic pathways of the cross-feeding prokaryotes offering ATP path efficiency returns on a basis of economic division of labour.

The most significant biophysical structural limitation for the prokaryotic cell arises from how its bioenergetics are integrated with the cell membrane (see Fig 1).

This creates a limit to the bioenergetic capacity of a prokaryotic cell due to the limits imposed by the surface area of the cell membrane. This bioenergetic limitation has resulted in practical limits on the genome size and hence information capacity of prokaryotes.

In comparison, eukaryotes whose possession of mitochondria with their folded membranes have a much higher surface area for their bioenergetics and hence can sustain a larger genome. This emerged as the evolutionary 'solution' to restricted bioenergetic capacity and restricted information capacity in prokaryotes (Lane and Martin, 2007; Lane and Martin, 2012, Lane, 2015).

Lane and Martin's hypothesis has been questioned notably by Lynch and Marinov (2015,2016,2017), with Lynch subscribing to the view that natural selection is overemphasized and is_not the main evolutionary driver of emergent physical structural complexity in biology. He instead, argues it arises from genetic drift and mutation (Lynch, 2007). Schavemaker and Muñoz-Gómez (2022) reviewed Lynch and Marinov's data in the context of cell form and function,) reporting that it supports Martin and Lane's hypothesis in the case of larger cells.

*This is of course where the crux of the information -resource debate rests.*

There are bioenergetic constraints for prokaryotic cells below a certain volume to surface area and for faster growing (replicating) prokaryotic cells at larger genome sizes (Schavemaker &Muñoz-Gómez, 2022). Schavemaker and Muñoz-Gómez conclude that larger eukaryote genomes really need the bioenergetic capacity offered by mitochondria (Schavemaker &Muñoz-Gómez, 2022).

This paper also challenges Lynch's view in its presentation of biophysical systems examples of how prokaryote natural selection is driven by competition for resources and space; against biophysical limitations on form and function in the context of survival challenges arising from the environment.

With reference to the case study provided below, if there were such a weak linkage between natural selection of prokaryotes and their environmental adaptation as Lynch implies, the prokaryote extended phenotype case study would not be expected to report such a strong linkage between physical form and function in respect of successful replication and persistence within the case study environment alongside the spread and conservation of those shared traits amongst diverse prokaryote phenotypes within that prokaryote community.

Resource efficiency tactics are coded into many prokaryote genomes and the evolution of resource efficiency has also been a driver for the emergence of *increased information utilization efficiency* in the prokaryote genotype and phenotype.

*Information system evidence for evolutionary feedback into development of information utilization efficiency*

Prokaryote cell genome size is ultimately limited by prokaryote physical cell form and function constraints. Information utilization is a process towards a goal, which for life is defined as *system replication* (as per definition above). On that basis, regulation of gene expression represents a critical development in the information utilization efficiency of the prokaryote genotype and phenotype in meeting the challenges to replication set by any given environment.

Thermodynamic constraints lead cellular life to reproduce on the basis of fastest rate of individual cell reproduction ('r' reproduction strategy) if the environment is unlimited in resources, or under resource limitation conditions, reproduction on the basis of optimized yield and optimized resource efficiency will tend to be preferred. Thermodynamic constraints can set the threshold for whether a species is likely to establish itself in an environment in which competition for resources exists (Seto, 2014).

The prokaryote genome is structured and regulated on a basis that is inherently resource efficient and information efficient (*e.g.* Struhl, 1999). Metabolic pathway genes are grouped in a cluster – the operon- which has common regulatory control such that gene expression is not just synchronized but rapid. Some environmental stresses induce complex regulation via gene cascades. The genes that encode environment relevant information related to catabolism, metabolism and reproduction are inducible, meaning that presence or absence of a chemical species in the environment leads to their activation.

Within prokaryote metabolism, information system efficiency is increased by catabolism-induced genes being inducible and hence being switched on when the encoded catabolic substrate is present in the cytoplasm and environment. In contrast and further maximizing resource efficiency, anabolic genes are repressed while any anabolic product is still present in the cell cytoplasm so conserving resources. If more than one catabolic substrate is encoded for and is present in the environment and cytoplasm, then the prokaryote genome typically selects the highest survival-potential substrate first (*e.g* E. coli and the LAC operon (Jacob &Monod, 1962)).

Prokaryote transcription level regulation allows for rapid response to critical environmental change and its systems logic 'reads' like a best practice manual for readily and resource efficiently managing risks to reproduction of the prokaryote genotype in any environment.

The sophistication and complexity of how the survival and the reproduction relevant information maintained in prokaryote genomes is managed and utilized is high, as would be expected from a physical-information system point of view for over 3 billion years of prokaryote evolution stochastically exploring different environmental challenges.

The structural sophistication of prokaryotes is ultimately limited by the upper genome size a prokaryotic cell can reproduce. That limitation is likely to have been the driver for 'learning -system exploration' of the catabolic opportunity space – and may have been responsible for the emergence of huge diversity in catabolism in prokaryotes.

Competition for space to reproduce into, translated into material resource use innovation, also leads to niche environment exploitation. Diversity in catabolic substrate and its reactants allows new environmental niches to be explored. Niche environment colonization can itself be internally exploited based on an 'r' reproductive strategy or a 'K' reproductive strategy depending on the bioenergetic returns possible in the 'niche' environment.

Prokaryotes reproduce vegetatively, i.e. daughter cells are clones of parent cells. A key factor in *information utility* for a replicator is a source of information variation to allow system development innovation. Variation in information for prokaryotes arises from mutation and genetic drift (including gene loss) as well as through recombination. Metabolic gene loss mutants are favoured by adaptative fitness benefits when the environment contains the require metabolites (De Souza & Kost, 2016).

Within prokaryotes, the emergence of recombination via various forms of Horizontal Gene Transfer HGT) has allowed for significant information transfer between different prokaryote phenotypes. HGT as a process puts information at risk as transfer operations include viral transduction and conjugation to transfer plasmids where the agents of recombination would be expected to have their own self-interest in being replicated. Negative outcomes range from acquisition of unharmful genetic parasites (which in a prokaryote genome with a limited information capacity represents loss of valuable information space) to acquisition of genes that harm replicative success.

Despite this, HGT is widespread in prokaryotes and some prokaryotes have mechanisms promoting HGT and HGT can influence cooperation and conflict between prokaryote phenotypes (Hall *et al*, 2020) . It seems likely that as a prokaryote habitat becomes more challenging, stress on system replication also increases the value for information system variation within the prokaryote phenotype, notably if the existing genome is not equipped to deal with the emergent stressors.

Resource challenges, from substrate availability and its variation to securing living space, have led to the emergence of significant diversity in catabolic substrate exploitation in prokaryotes, but prokaryote sophistication extends much further than that.

Competition in securing resources from information utilization efficiency is an evolutionary driver for the emergence of sensing in prokaryotes. The significance of the emergence of prokaryote sensing is that *it creates a basis for improved information utilization within an individual cell/individual phenotypes life cycle.*

*With sensing coupled to regulation, adaptation is not just occurring between generations but within an individual prokaryote phenotypes' life cycle.*

Quorum sensing fulfills a prokaryote resource management purpose in relation to attempting to maximize replicative success through utilization of environmental information (Kreft, 2004; Costa *et al*, 2006, Hense *et al*, 2007). When resources become limited or variable, an anabolic strategy that

maximizes *resilience of the species* is required to maximize prokaryote genotype survival, where symbiotic resource tactics as well as tactics for resource competition play a role.

The limitations on prokaryotes genome size have restricted the physical structural complexity that could be developed within prokaryotic cells. This may be the reason why 'division of labour resource economy 'structures within the prokaryotic cell such as that provided by organelles occurred until the emergence of eukaryotic cells with mitochondria from an archaeal/eubacterial symbiosis.

Physical limitations of the prokaryotic cell phenotype have confined prokaryotic multicellular growth for a single species of prokaryote to one form, 'filamentous' growth, in which linear, linked vegetative reproduction forms a filament.

However, there are also examples in nature of prokaryote cooperative and competitive multicellular growth for mixed species growth, in a prokaryotic example of a common extended phenotype that has emerged in aqueous environments.

*Case study: the wastewater prokaryote extended phenotype*

An extended phenotype is defined by Dawkins as the wider effect the phenotype of an organism or species can have on its environment, through interactions with its environment that extend beyond the direct mechanical capabilities of its physical phenotype.

*Two general forms of extended phenotype are thought possible (Hunter, 2018):*

A species physically conforms its environment to favour its survival and reproduction. The classic example used is the beaver and the beaver pond, which other organisms may benefit from, but the beaver's reason for reforming part of its environment to its own specification is based on reproductive self-interest,

Two organisms interact in a relationship where one locally manipulates the behaviour of the other such as a parasite-host interaction; or a subset of individual phenotype interaction where the two organisms influence each other at a distance.

In this wastewater case study, we will examine a prokaryote version of the first 'beaver pond' form of extended phenotype that emerged in prokaryotes in an aquatic type of environment.

The municipal wastewater environment is typically resource limited and rather variable in substrate concentration terms as well as being a flow -through environment. This leads to two predominating natural selection pressures for municipal wastewater prokaryotes: starvation and washout.

Starvation risk management is the most likely purpose for the evolution of quorum sensing in the wastewater prokaryote extended phenotype.

The environment varies in its substrate concentrations, so the heterotrophic bacteria typically associated with the habitat have developed significant catabolic range and diversity in their phenotype and are able to catabolize dissolved organic carbon aerobically and anoxically when oxygen is limited.

This includes an ability to rapidly uptake the most bioenergetically advantageous organic carbon substrates and convert some to intracellular food reserves.

When the primary catabolic substrates are absent, this phenotype includes a capability for shifting resources to production of hydrolytic enzymes to break down particulate volatile solids near the cell. After those resources are exhausted, this heterotrophic phenotype can then shift anabolic activity to maintenance and endogenous respiration.

This diversity in the catabolic phenotype optimizes survival to replication probability in this environment. This cycle of catabolic resource management is seen globally in aerobic municipal wastewater treatment systems daily. (Fig 3).

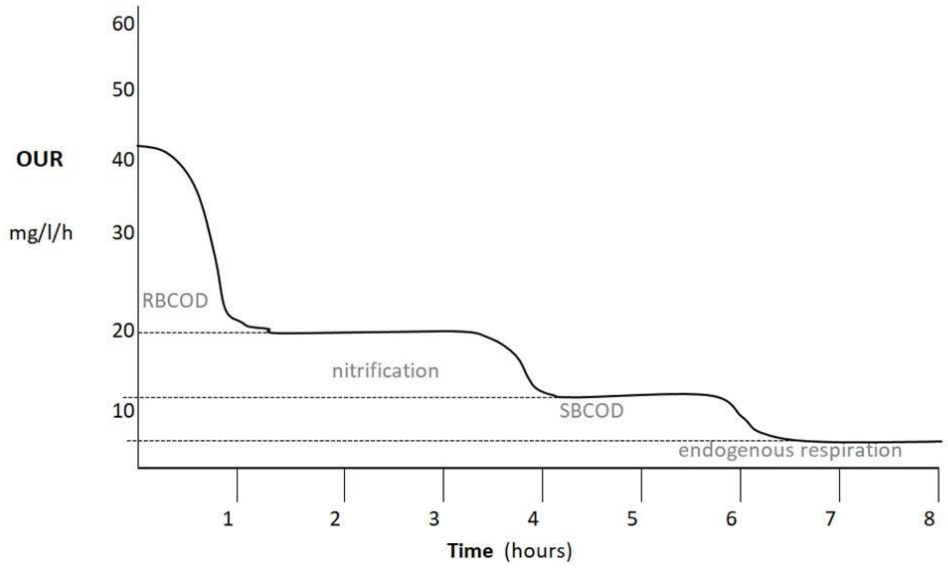


*Figure 3:* The municipal wastewater prokaryote extended phenotype

The typical municipal wastewater Oxygen Uptake rate for activated sludge systems shows stages of oxygen demand, with three stages in carbonaceous treatment systems and four stages for biotreatment systems designed with a longer mean cell residence time to accommodate slower growing ammonia oxidising and nitrite oxidising prokaryotes. The wastewater extended phenotype heterotrophic prokaryotes dominate oxygen demand due to their better bioenergetic returns on catabolism until their soluble substrates are exhausted. This phenotype then initiates comparatively expensive biosynthesis of hydrolytic enzymes to release more dissolved organic carbon from any local sources of volatile solids. In this period, the slower growing nitrifiers now dominate oxygen removal for ammonia oxidation until ammonia levels reach system equilibrium, at which point the oxygen demand associated with hydrolysed Slowly Biodegradable COD (SBCOD) occurs. After hydrolysed SBCOD has been oxidized, the municipal wastewater extended phenotype shifts to endogenous respiration).

The municipal wastewater extended phenotype includes a quorum sensing capability (Chong *et al,* 2012) that allows the phenotype to sense the local ratio of catabolic substrate to cell.

Below a threshold value which implies reactive resource scarcity, quorum sensing to initiate a K reproductive strategy allows optimized resource efficiency (Hense *et al*, 2007) and optimized resource acquisition capability. The heterotrophic prokaryotes with this phenotype switch to a high uptake rate of acetate and begin to produce External Polymeric Substances (EPS). The ability to produce EPS in this form is likely to have arisen from the genotype for competitive rapid uptake of acetate undergoing mutations and/or gene loss, or recombination, to provide phenotype restructuring towards acetate being shifted into EPS formation outside the cell.

The advantage of this phenotype with external resource storage that would immediately feed back into survival towards replication, is that there are now no space limits within the cell to stop the phenotype accumulating its optimum substrate from the environment while it is available (Palmer *et al*, 2020). Consequently, a structural material (EPS) is formed outside cells of this phenotype. *This minor*

*structural change in phenotype also turns out to confer additional significant advantages towards survival directed to replication, including:*
EPS facilitates cell aggregation which allows cells of this phenotype to form associations, also creating opportunities for cooperative resource acquisition (Rainey & Rainey, 2003), (Kreft, 2004), (Flemming *et al*, 2016) also reducing the survival risk profile for the phenotype(Boles *et al*, 2004);

- Aggregated growth occurs as biofilm in lower substrate environments and as flocs or granules where aggregated growth can settle under gravity at the upflow rates through that environment.
- What was likely to have originally observed as a starvation management tactic also provides mitigation against phenotype wash-out from the system (Palmer *et al*, 2020),
- The EPS layer entraps particulate material, *reducing the risk* of the phenotype investing in hydrolytic enzyme production once its primary soluble substrates are locally exhausted, as EPS particulate capture makes local particulate VSS highly likely,
- The EPS layer provides a location for growth of other prokaryotes including nitrifiers. Any local nitrate production in a mixed growth system provides this municipal wastewater extended phenotype with a possible diversification of catabolism of their primary substrates via anoxic catabolism,
- The EPS layer traps DNA and increases the probability of information variation via HGT (Merod & Weurtz, 2014) for this phenotype.

*This extended phenotype is spread across several species and genera that proliferate in this particular environment.*

In order to replicate its genome through successive generations, the phenotype as a vehicle for replication needs to optimize resource acquisition and manage resource paucity. The municipal wastewater extended phenotype presented in this case study is a good example of how minor genetic variation in a resource stressed environment can lead to a range of benefits with complex biological system behavior emerging from a single phenotypic attribute and significantly changing the phenotype's relationship with its environment due to that change locally reconfiguring the phenotype's environment.

*Origin of Life: new insights from thermodynamics systems analyses*

Physical system analysis is now being applied to the emergence of life on Earth. Hypotheses for the emergence of Life on Earth have for some time included an alkaline hydrothermal vent geological origin for life (Martin & Russell, 2003; Lane, 2015). This hypothesis assumes autotrophic methanogenesis as the basis for the emergence of bioenergetic catabolism:

$$CO_2 + 4H_2 \rightarrow CH_4 + 2H_20$$

Recent research deeper into this hypothesis has included thermodynamic analysis which provides critical contextual insight into what is physically possible.

One paradox for emergence of life is how the agent of memory – genetic code, emerges at the same time as a functional metabolism providing exergy for both code and energy source replication if an 'RNA world hypothesis is followed. More recent hypotheses retain RNA as the initial critical information system but more deeply examine how that is possible for life emerging from a geochemical origin.

On a physical system basis, a geochemical system possessing a boundary layer is profoundly different to one with no boundary. A simple fatty acid/lipid boundary layer creates a semi-permeable barrier that can facilitate differentiation between an internal environment for the emergent biological system

and the systems external environment. A semi-permeable boundary structure provides a basis for chemical gradients that can foster metabolise to replace geochemical energy sources and a semi-permeable boundary structure also creates an internal surface for reaction chemistry and initial internal structure development Wimmer *et a*l (2016),(Palmeira *et al*, 2022; Harrison *et al*, 2022).

Consequently, a semipermeable protocell is a structure that can facilitate development of a metabolism to drive replication of the system independent of any geochemistry the system emerged from. A semi-permeable fatty acid/lipid boundary structure also provides a physical structure which could self-replicate in an aqueous system, with volume to surface area of the structure giving a basis for division of the boundary Corominas-Murtra (2019).

These factors are now issues to examine in assessment of the emergence of life from a geochemical source because very recent breakthroughs have been made in understanding the physics (thermodynamics) and chemistry. Wimmer *et a*l (2016) reported on their systematic review of the physical chemistry now assumed for LUCA, which identified that the principal biosynthetic associated with its metabolism could be provided by hydrothermal vent conditions.

Autotrophic methanogenesis creates larger metabolites than its catabolic substrate which means it is entropy decreasing and this results in its driving $\Delta_r G$ being enthalpy ($\Delta_r H$) dominated. The energy dissipation of this reaction is far larger and more enthalpy driven than the aerobic respiration represented in Fig. 1. When the ratio of catabolic enthalpy $\Delta_r H$ to catabolic driving force $\Delta_r G$ is plotted for the known range of types of catabolic reactions and their driving forces ((von Stockar, 2013) all prokaryote metabolic regimes have a ratio of 1 or less, with the lone exception of autotrophic methanogenesis which has a ratio over 4. This significant thermodynamic distance from other metabolism clearly identifies autotrophic methanogenesis as a thermodynamic candidate for the emergence of prokaryotic life from a geochemical 'cradle' as described by Wimmer *et a*l (2016).

More recently, Corominas-Murtra (2019) investigated the thermodynamics of the duplication of lipid cells and determined that duplication required a balance between supply of exergy (free energy) and entropic forces associated with lipid boundary and sphere growth and maintenance up to the point of sufficient resources for its duplication. This work showing that protocell emergence requires a thermodynamic window, provides support for two studies showing how autotrophic protometabolism could develop in an alkaline hydrothermal vent environment and lead to the production of protocells (Palmeira *et al*, 2022; Harrison *et al*, 2022).

These thermodynamic system analyses have identified a development route by which protocells with autotrophic protometabolism, in which autocatalytic nucleotide synthesis and $CO_2$ fixation drive growth and protocell replication.

This route for the emergence of life starts with a geochemical environment that provides the chemistry and enthalpy required to support autotrophic metabolism, which in turn in that environment produces lipid-bound protometabolic in which nucleotides play a critical role. This provides a replicable protocell within which RNA can form (Palmeira *et al*, 2022; Harrison *et al*, 2022).

## IV. CONCLUSIONS

Physical systems analysis of biological systems provides insights into the physical mechanisms that life both acts on and is defined by and the critical role played by the environment. Life and biological systems are distinguished from biological and chemical systems by their attribute of memory, the agent of which is the gene.

Using the physical definition of life provided in this paper:

*'A c system with memory which is utilized for environmental fitness, with fitness defined by success in replicating that system.'*

Lynch's contention that natural selection plays a minimal role in biological evolution and in the emergence of the complexity observed in biological systems (Lynch, 2007) cannot be reconciled with how biology works in physical terms as explained in this paper.

Complexity arises even in simple systems if they have sustained positive feedback over generations (Kaufmann, 1996; Holland, 1992, Holland 1996, Holland 1998).

In the case of biological systems, the purpose of information storage, i.e. memory (genotype), is for reproduction. The physical context for any use of information is that system information's distinguishability between the system and its environment.

For biological systems their purpose is self-replication and their environment and their alignment to it determines their reproductive success. Extinction of a genotype is the price of the failure of a phenotype to achieve the minimum level of resource management through information utilization required to successfully replicate its genome. For biological systems, the definition of information (compared to noise or misinformation), is accurate environment-relevant data.

Reproduction requires material resources and energy resources which have to be obtained from the environment which will usually include competitors for those resources. Biological system complexity arises from the need to optimize replication through securing resources needed for it. The phenotype is the physical structural information arising from genome replication and expression needed to secure the energy and material resources needed to sustain and reproduce a biological system. There is continuous positive system feedback between a genome and the environment through the phenotype's ability to secure all the resources, including space, needed to continue to replicate the genome.

The prokaryote genome often encodes information for two reproductive strategies that map directly to the ecological theory of 'r' strategy reproduction (maximum rate of reproduction of offspring) and 'K' strategy (lower rate of reproduction of more resilient offspring) and this in turn includes sensing based regulation which represents information utilization by the genome in expressing a phenotype within the organism's lifetime.

Sensing emerged in prokaryotes to satisfy basic physical requirements of reproduction. Quorum sensing emerged as the basis for prokaryotes to shift phenotype between an ''r' reproductive strategy or a 'K' reproductive strategy. Although these reproductive strategies have fallen out of favour for use in large, complex eukaryote ecology, this paper shows how both strategies arise from biophysical constraints in prokaryotes and emerge early in the evolution of life on Earth. In prokaryotes at least, 'r' strategy and 'K' strategy exactly describe how reproduction is tailored to environment resource opportunity or limitation and the characteristics (Reznick *et al*, 2002) attributed to each strategy in ecology fit well to prokaryote use of r' or 'K' strategy for reproduction in their microenvironments. For more complex organisms 'r' strategy and 'K' strategy might be expected to provide a less accurate fit to observed behaviour but for prokaryotes and microorganisms. Secondly, ecological analyses have until recently lacked systems analyses that took into account the significance of non-Markovian processes in biology in forming a view resource appreciation in reproductive strategy formulation, but such

approaches such, as discounted reproductive number (Reluga *et al*, 2009) are now available and may help encourage increased use of r' and 'K' strategy in future.

Resource acquisition strategies and tactics in biology are central to early ecology and are critical physical challenges for all biological systems to manage within their relationship to their environment in order to optimize genome replication. The systems behaviour we describe as 'economics' appears in biological resource acquisition strategies and tactics emerging in prokaryotes described in this paper.

## ACKNOWLEDGEMENTS

The author has no conflicts of interest to declare.

## REFERENCES

1. Ben Naim, A. (2008) A Farewell to Entropy: Statistical Thermodynamics based on information. Publ. World Scientific Publishing Co. Pte Ltd UK. ISBN: 978-981-270-707-9.
2. Palmer, S.J. (2019). A review of the physical roles of information in nature. Journal of Biological Physics and Chemistry. Vol 19 p22-40 (2019).
3. Tribus, M. and McIrvine, E.C. (1971). Energy and information. Scientific American, September 225, 179–188.
4. Holland, J.H. (1992) Adaptation in Natural and Artificial Systems: An Introductory Analysis with Applications to Biology, Control and Artificial Intelligence (Complex Adaptive Systems). mergence: from chaos to order. MIT Press. ISBN 978-0262581110.
5. Holland, J.H. (1998) Emergence: from chaos to order. Oxford University Press. ISBN 978-0-19-286211-2.
6. Holland, J.H. (1996) Hidden Order: How Adaptation Builds Complexity. Basic books/Perseus Books Group. ISBN 0-201-44230-2.
7. Dawkins, R. (1976). The Selfish Gene (first edition). Oxford University Press. ISBN 0-19-857519-1
8. Dawkins, R. (1982) The Extended Phenotype: the long each of the gene. Oxford University Press. ISBN 0-19-288051-9.
9. Martin, W. Russell, M.J. (2003) On the origins of cells: a hypothesis for the evolutionary transitions from abiotic geochemistry to chemoautotrophic prokaryotes, and from prokaryotes to nucleated cells. Phil. Trans. R. Soc. Lond. B 2003 358, p59-85.
10. Lane, N. (2015). The Vital Question: Why is life the way it is? Publ. Profile Books Ltd (2015, 2016). ISBN 978 1 78125 037 2.
11. von Stockar, U. (2013) Live cells as open non-equilibrium systems. Chapter 16, 399-421. In: von Stockar, U. (ed)(2013. Biothermodynamics: the role of thermodynamics in Biochemical Engineering. EPFL Press 1st edition (2013).
12. Heijnen, J.J. (2013) A thermodynamic approach to predict black box model parameters for microbial growth. Chapter 18, 443-473. In: von Stockar, U. (ed)(2013. Biothermodynamics: the role of thermodynamics in Biochemical Engineering. EPFL Press 1st edition (2013).
13. Wang, G., Post, W.M. (2012). A theoretical reassessment of microbial maintenance and implications for microbial ecology modelling. FEMS Microbiol. Ecol. 81p610-617.
14. Reznick, D., Bryant, M.J., Bashey, F. (2002) Ecology 83(6) p1509-1520.
15. Monod, J. (1950) La technique de culture continue. Théorie et applications.. Ann. Inst. Pasteur. 79. p390-410.
16. Herwig Bachmann, H., Bruggeman, F.J., Molenaar, D., dos Santos, F.B., Teusink, B. (2016) Public goods and metabolic strategies. Current Opinion in Microbiol. 31p109-115.
17. Bradley, J.A., Amend, J.P., LaRowe, D.E. (2018) Survival of the fewest: Microbial dormancy and maintenance in marine sediments through deep time. Geobiology 17: p43-59.

18. De mattos, M.J.T.., Neijssel, O.M. (1997) Bioenergetic consequences of microbial adaptation to low-nutrient environments. Journ. Biotech. 59 p117-126.
19. Gonzalez,O., Gronau, S., Pfeiffer, F., Mendoza, E., Ralf Zimmer, R., Oesterhelt, D. (2009) Systems analysis of the Bioenergetics and Growth of the Extreme Halophile *Halobacterium salinarum* PLOS Comp. Biol. 5 (4) p1-11.
20. Costa E., Perez J., Kreft ,J.U. (2006) Why is metabolic labour divided in nitrification? Trends Microbiol 14: 213-219.
21. Lane, N and Martin, W. (2007) The energetics of genome complexity. Nature. Vol. 467 p929-934.
22. Lane, N. and Martin, W.F. (2012). The origin of membrane bioenergetics. Cell 151, 1406–1416.
23. Lynch, M. (2007) The frailty of adaptive hypotheses for the origins of organismal complexity. Proc. Nat. Acad. Sci. 104(Suppl 1):8597-8604.
24. Lynch, M., Marinov, G.K. (2015) The bioenergetic costs of a gene. Proc. Nat. Acad. Sci. 112(51):15690-15695.
25. Lynch, M., Marinov, G.K. (2016) Reply to Lane and Martin: Mitochondria do not boost the bioenergetic capacity of eukaryotic cells. PNAS 11113 E667-E668.
26. Lynch, M., Marinov, G.K. (2017) Membranes, energetics and evolution across the : prokaryote-eukaryote divide. eLife, 6 e20437.
27. Schavemaker, P.E., Muñoz-Gómez, S.A. (2022) The role of mitochondrial energetics in the origin and diversification of eukaryotes. Nat Ecol Evol 6, 1307–1317 (2022). https://doi.org/10.1038/s41559-022-01833-9.
28. Jacob, F., & Monod, J. On the regulation of gene activity. Cold Spring Harbor Symp. Quant. Biology 26, 193–211 (1962).
29. Struhl, K. (1999) Fundamentally different logic of gene regulation in eukaryotes and prokaryotes. Cell 98, 1-4.
30. Seto, M. (2014) The Gibbs free energy threshold for the invasion of a microbial population under kinetic constraints. Geomicrobiology Journ. 31, 645-653.
31. De Souza, G., Kost, C. (2016) Experimental evolution of metabolic dependency in bacteria. LPOS genetics DOI: 10.1371/journal.pgen.1006364.
32. Hall, R.J., Whelan, F.J., McInerney J.O., Ou Y,Domingo-Sananes, M.R. (2020) Horizontal gene transfer as a source of conflict and cooperation in prokaryotes. Frontiers in Microbiology, 17 Jul 2020, 11:1569 DOI: 10.3389/fmicb.2020.01569.
33. Hense, B., Kuttler, C., Müller, J., Rothballer, M., Hatmann, A., Kreft ,J.U. (2007) Does efficiency sensing unify diffusion and quorum sensing?. Nat Rev Microbiol 5, 230–239 (2007). https://doi.org/10.1038/nrmicro1600.
34. Hunter, P. (2018) The revival of the extended phenotype. EMBO Reports 19:e46477 DOI: 10.15252/embr.2018464477.
35. Chong, G., Kimyon, O., Rice, S.A., Kjelleberg, S., Manefield, M. (2012). The presence and role of bacterial quorum sensing in activated sludge. Microbial. Biotech. 5(50, p621-633.
36. Palmer, S.J., Noone, G., Hoyland, G. (2020).A review of the physical relationships between form and function in wastewater biotreatment biophysical relationships and a new theory relating activated sludge and biofilm systems behaviour. Water and Env. Journ. Doi:10.1111/wej.12614.
37. Rainey, P.B., Rainey, K. (2003) Nature Letters Vol 425 4 Sept 2003 p72-74.
38. Kreft ,J.U. (2004) Biofilms promote altruism. Microbiology 150: 2751-2760.
39. Flemming, H-C., Wingende, J., Szewzyk, U., Steinberg, P., Rice, S.A., Kjelleberg, S. (2016) Biofilms: an emergent form of bacterial life. Nature Reviews 14, 563-574.
40. Boles, B.R., Thoendel, M., Singh, P.K. (2004) Self-generated diversity produces “insurance effects” in biofilm communities. PNAS 101 (47) 16630-16635 https://doi.org/10.1073/pnas.0407460101

41. Merod R.T., Weurtz, S., (2014)Extracellular Polymeric Substance Architecture Influences Natural Genetic Transformation of *Acinetobacter baylyi* in Biofilms. Appl. Environ. Microbiol. 80 (24) p7752-7757
42. Corominas-Mutra B (2019) Thermodynamics of Duplication Thresholds in Synthetic Protocell Systems. Life 9 (9) DOI:10.3390/life9010009
43. Wimmer, J.L.E., Xavier, J.C., Vieira A.N, Pereira, D.P.H., Leidner, J., , Sousa, F.L., Kleinermanns, K., Martina Preiner., M., Martin, W.F. (2021) Energy at Origins: Favorable Thermodynamics of Biosynthetic Reactions in the Last Universal Common Ancestor (LUCA). Frontier in Microbiol. 12 p1-18 DOI 10.3389/fmicb.2021.793664
44. Nunes Palmeira R, Colnaghi M, Harrison SA, Pomiankowski A, Lane N. The limits of metabolic heredity in protocells. Proc Biol Sci. 2022 Nov 9;289 (1986):20221469. doi: 10.1098/rspb.2022.1469. Epub 2022 Nov 9. PMID: 36350219; PMCID: PMC9653231.
45. Harrison, Stuart A; Palmeira, Raquel Nunes; Halpern, Aaron; Lane, Nick; (2022) A biophysical basis for the emergence of the genetic code in protocells. Biochimica et Biophysica Acta (BBA) - Bioenergetics , Article 148597. 10.1016/j.bbabio.2022.148597.
46. Kauffman, S. (1996) At Home in the Universe: The Search for the Laws of Self-Organization and Complexity. Oxford University Press (USA). ISBN 978-0195111309
47. Reluga, T.C., Medlock, J., Galvani, A. (2009) Math. Biosciences & Eng. 6(2)p377-393